Article

Cell Metabolism

Selenium mediates exercise-induced adult neurogenesis and reverses learning deficits induced by hippocampal injury and aging

Graphical abstract

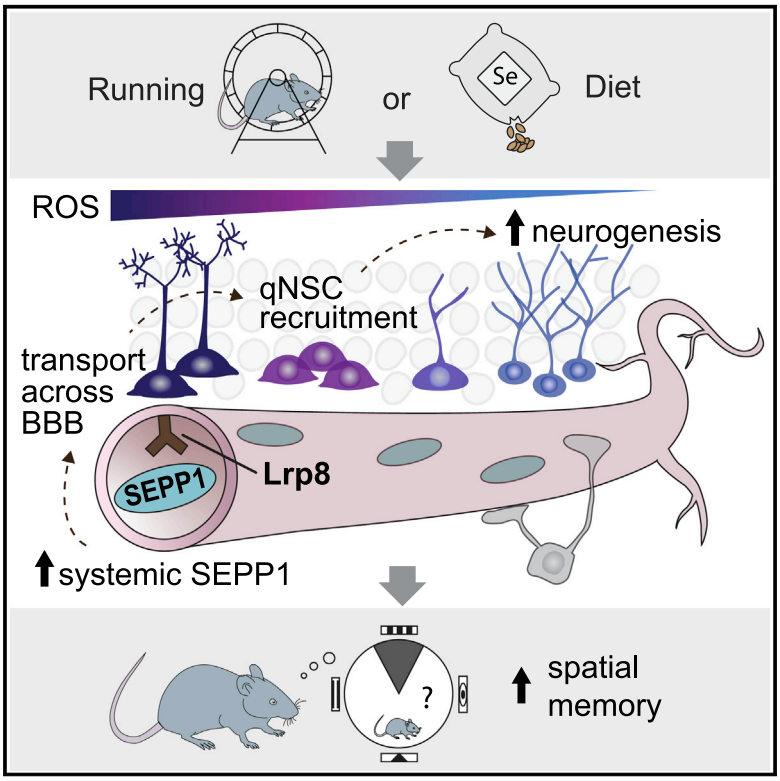

Authors

Odette Leiter, Zhan Zhuo, Ruslan Rust, ..., Sheng-Tao Hou, Gerd Kempermann, Tara L. Walker

Correspondence

hou.st@sustech.edu.cn (S.-T.H.), gerd.kempermann@dzne.de (G.K.), t.walker1@uq.edu.au (T.L.W.)

In brief

Exercise increases new neuron generation in the hippocampus, a brain region with important learning and memory functions. Here, Leiter et al. report that this process is mediated by an increase in systemic selenium transport. Dietary selenium supplementation restored neurogenesis and reversed cognitive decline in aging and in a model of hippocampal injury, suggesting potential therapeutic relevance.

Highlights

- Selenium mediates the exercise-induced increase in adult hippocampal neurogenesis
- Selenium increases hippocampal precursor proliferation and adult neurogenesis
- Selenium reverses cognitive decline in aging and in hippocampal injury

Leiter et al., 2022, Cell Metabolism *34*, 408–423
March 1, 2022
https://doi.org/10.1016/j.cmet.2022.01.005

CellPress

CellPress
OPEN ACCESS

Cell Metabolism

Article

Selenium mediates exercise-induced adult neurogenesis and reverses learning deficits induced by hippocampal injury and aging

Odette Leiter,[1,2,3,8] Zhan Zhuo,[1,4,8] Ruslan Rust,[2,3,10] Joanna M. Wasielewska,[2,3] Lisa Grönnert,[2,3,11] Susann Kowal,[2,3] Rupert W. Overall,[2,3] Vijay S. Adusumilli,[2,3] Daniel G. Blackmore,[1] Adam Southon,[5] Katherine Ganio,[6] Christopher A. McDevitt,[6] Nicole Rund,[2,3] David Brici,[1] Imesh Aththanayake Mudiyan,[1] Alexander M. Sykes,[7] Annette E. Rünker,[2,3] Sara Zocher,[2,3] Scott Ayton,[5] Ashley I. Bush,[5] Perry F. Bartlett,[1] Sheng-Tao Hou,[4,*] Gerd Kempermann,[2,3,9,*] and Tara L. Walker[1,2,3,9,12,*]

[1]Queensland Brain Institute, The University of Queensland, Brisbane, Australia
[2]CRTD – Center for Regenerative Therapies Dresden, Technische Universität Dresden, Dresden, Germany
[3]German Center for Neurodegenerative Diseases (DZNE) Dresden, Dresden, Germany
[4]Brain Research Centre and Department of Biology, Southern University of Science and Technology, Shenzhen, China
[5]The Melbourne Dementia Research Centre, The Florey Institute of Neuroscience and Mental Health, University of Melbourne, Melbourne, Australia
[6]Department of Microbiology and Immunology, The Peter Doherty Institute for Infection and Immunity, The University of Melbourne, Melbourne, Australia
[7]Max Planck Institute for Molecular Cell Biology and Genetics, Dresden, Germany
[8]These authors contributed equally
[9]These authors contributed equally
[10]Present address: Institute for Regenerative Medicine (IREM), University of Zurich, Zurich, Switzerland
[11]Present address: Pharmaceutical Research and Early Development, Ocular Technologies, I2O, Roche Innovation Center Basel, F. Hoffmann-La Roche Ltd., CH-4070 Basel, Switzerland
[12]Lead contact
*Correspondence: hou.st@sustech.edu.cn (S.-T.H.), gerd.kempermann@dzne.de (G.K.), t.walker1@uq.edu.au (T.L.W.)
https://doi.org/10.1016/j.cmet.2022.01.005

SUMMARY

Although the neurogenesis-enhancing effects of exercise have been extensively studied, the molecular mechanisms underlying this response remain unclear. Here, we propose that this is mediated by the exercise-induced systemic release of the antioxidant selenium transport protein, selenoprotein P (SEPP1). Using knockout mouse models, we confirmed that SEPP1 and its receptor low-density lipoprotein receptor-related protein 8 (LRP8) are required for the exercise-induced increase in adult hippocampal neurogenesis. *In vivo* selenium infusion increased hippocampal neural precursor cell (NPC) proliferation and adult neurogenesis. Mimicking the effect of exercise through dietary selenium supplementation restored neurogenesis and reversed the cognitive decline associated with aging and hippocampal injury, suggesting potential therapeutic relevance. These results provide a molecular mechanism linking exercise-induced changes in the systemic environment to the activation of quiescent hippocampal NPCs and their subsequent recruitment into the neurogenic trajectory.

INTRODUCTION

Adult hippocampal neurogenesis is an evolutionarily conserved process that provides a particular type of structural plasticity to the brain, allowing life-long flexibility that supports effective learning and memory. Although there is strong evidence that this process is found in humans where it is thought to underlie cognitive processes critical for adaptive behavior (Boldrini et al., 2018; Moreno-Jiménez et al., 2019; Spalding et al., 2013; Tobin et al., 2019), we rely on animal studies to learn how the activity-dependent regulation of adult neurogenesis occurs at a mechanistic level. Although the two major adult neural stem cell niches in the hippocampal dentate gyrus (DG) and the subventricular zone (SVZ) of the lateral ventricles share many common features, it is becoming increasingly clear that they are under distinct regulatory control. One key difference between the neural precursor cells (NPCs) of these two neurogenic niches is their susceptibility to the induction of proliferation in response to physiological stimuli, such as physical exercise (Adusumilli et al., 2021; Brown et al., 2003). The broad range of effects of exercise across the body makes it likely that systemically released factors in the blood could serve as systemic

mediators of the neurogenesis-promoting effect. In support of this, a communication route via vessel-associated apical processes of radial glia-like stem cells has recently been described, which facilitates the direct access of systemic blood-borne factors exclusively into hippocampal neural stem cells (Licht et al., 2020).

In this study, we sought to identify systemic mechanisms by which exercise regulates adult hippocampal neurogenesis. As part of a previous study to identify proteins that are systemically released in response to exercise, we performed a proteomic screen on the blood plasma from mice that were housed in either standard cages or with a running wheel for 4 days (Leiter et al., 2019). We identified 68 proteins with significant running-induced changes in their plasma levels. Of these, selenoprotein P (SEPP1) was one of the most significantly upregulated proteins, present in the plasma of running mice at more than twice the level of controls (Figure 1A). Twenty-five mammalian selenoproteins, all of which contain selenocysteine residues, have been identified. However, among these SEPP1 is the most important for maintaining selenium levels in the brain. Unlike other selenoproteins that carry single selenocysteines, SEPP1 carries 10, one at its N-terminal domain with redox activity and nine at its C-terminal domain, which supply selenium to the brain via its receptor low-density lipoprotein preceptor-related protein 8 (LRP8) at the blood-brain barrier (Hill et al., 2007; Kurokawa et al., 2014; Burk et al., 2014). The activity-dependent increase in blood SEPP1 levels suggested a potential role of selenium in the activation of quiescent NPCs.

Here, we investigated whether a SEPP1-mediated increase in selenium transport underlies the exercise-induced increase in adult hippocampal neurogenesis. We also determined whether mimicking the effect of exercise by dietary selenium supplementation could restore neurogenesis and reverse the cognitive decline associated with aging and hippocampal injury.

RESULTS

Selenium increases NPC proliferation *ex vivo*

Having previously identified SEPP1 as one of the most significantly upregulated proteins in the blood of exercising mice (Leiter et al., 2019), we first used an ELISA-based approach to confirm that the 4-day running paradigm used in our initial mass-spectrometry-based proteomic screen resulted in a significant increase in plasma SEPP1 levels (Figure 1B). We also extended this analysis to reveal that a more acute bout of exercise (2-day running or 2 days of running followed by 2 days of standard housing) was similarly sufficient to increase plasma SEPP1 levels (Figure 1B).

Having established that systemic SEPP1 levels are significantly increased following exercise, we next investigated whether the treatment of NPCs with exogenous selenium also resulted in a subsequent increase in the proliferation of these cells using the *in vitro* neurosphere assay. This assay is a readout of proliferating precursor cells (Reynolds and Weiss, 1992). As the medium normally used to culture neurospheres from NPCs contains basal levels (30 nM) of the inorganic form of selenium, sodium selenite, we prepared the medium free of sodium selenite but otherwise as originally described (Reynolds et al., 1992). We found that significantly more neurospheres were generated from primary DG cells grown in the presence of 0.1 or 0.5 μM sodium selenite, compared with cells grown in the absence of selenium (Figure 1C). Selenium supplementation also significantly increased the number of neurospheres generated from primary cells isolated from the SVZ, the other major neurogenic region in the adult brain (Figure 1D). Neurosphere size is indicative of the proliferative potential of individual precursor cells, with larger neurospheres being generated from earlier precursors and small neurospheres being derived from more restricted progenitor cells (Walker et al., 2008). In addition to increasing the neurosphere number, a significant increase in the average neurosphere size and a greater prevalence of larger neurospheres (>150 μm in diameter) was observed following selenium supplementation (0.1 μM in the DG and between 0.05 and 1 μM in the SVZ; Figures 1E and 1F). Culturing cells in the presence of the organic form of selenium, seleno-L-methionine, produced similar results, increasing both the number and size of the neurospheres generated (Figures 1G–1J). The effect of selenium supplementation was direct, as precursor cells isolated using a lysophosphatidic acid receptor (LPA_1-GFP) reporter mouse line, which can be used to efficiently isolate a pure population of hippocampal precursor cells (Walker et al., 2016), showed a similar response in the absence of other niche cells (Figures 1K and 1L). The total number of NPCs in the hippocampal stem cell niche is a result of both the direct control of cell proliferation and the controlled elimination of daughter cells, many of which die within the first 4 days after division of the mother cell. This cell death occurs in two waves, an early phase 1–4 days after cell birth and a later phase at 1–3 weeks. We first confirmed that, although apoptosis does occur, selenium treatment did not alter the percentage of apoptotic (annexinV$^+$) NPCs in either adherent hippocampal precursor cultures (Figure S1A) or primary DG cells (Figure S1B). To confirm that selenium treatment was not toxic at the concentrations used in this study, we next used the Resazurin cell viability assay to quantify the number of viable adherent NPCs following treatment with 5 nM to 1 μM sodium selenite or seleno-L-methionine. This analysis revealed a small but significant increase in the number of viable cells in the adherent monolayer cultures supplemented with 0.5 or 1 μM sodium selenite (Figure 1M) or seleno-L-methionine (Figure 1N).

Following the induction of differentiation, we also found that significantly more βIII-tubulin$^+$ neurons were formed from primary DG-derived neurospheres that were generated under high-selenium conditions (0.1 and 0.5 μM) compared with those generated in the absence of selenium (Figure 1O). Similarly, selenium treatment increased the number of βIII-tubulin$^+$ neurons generated from SVZ-derived neurospheres at selenium concentrations of 0.05 and 0.1 μM (Figure 1P). Taken together, these findings indicate that selenium supplementation significantly increases NPC proliferation and neuronal lineage differentiation potential without affecting apoptotic cell death.

Selenium targets activatable NPCs *ex vivo*

We have previously identified two populations of precursor cells that can be activated by either potassium chloride (KCl) or norepinephrine (Jhaveri et al., 2010; Walker et al., 2008). As previously described, at basal selenium levels (30 nM), both KCl and norepinephrine significantly increased the number of

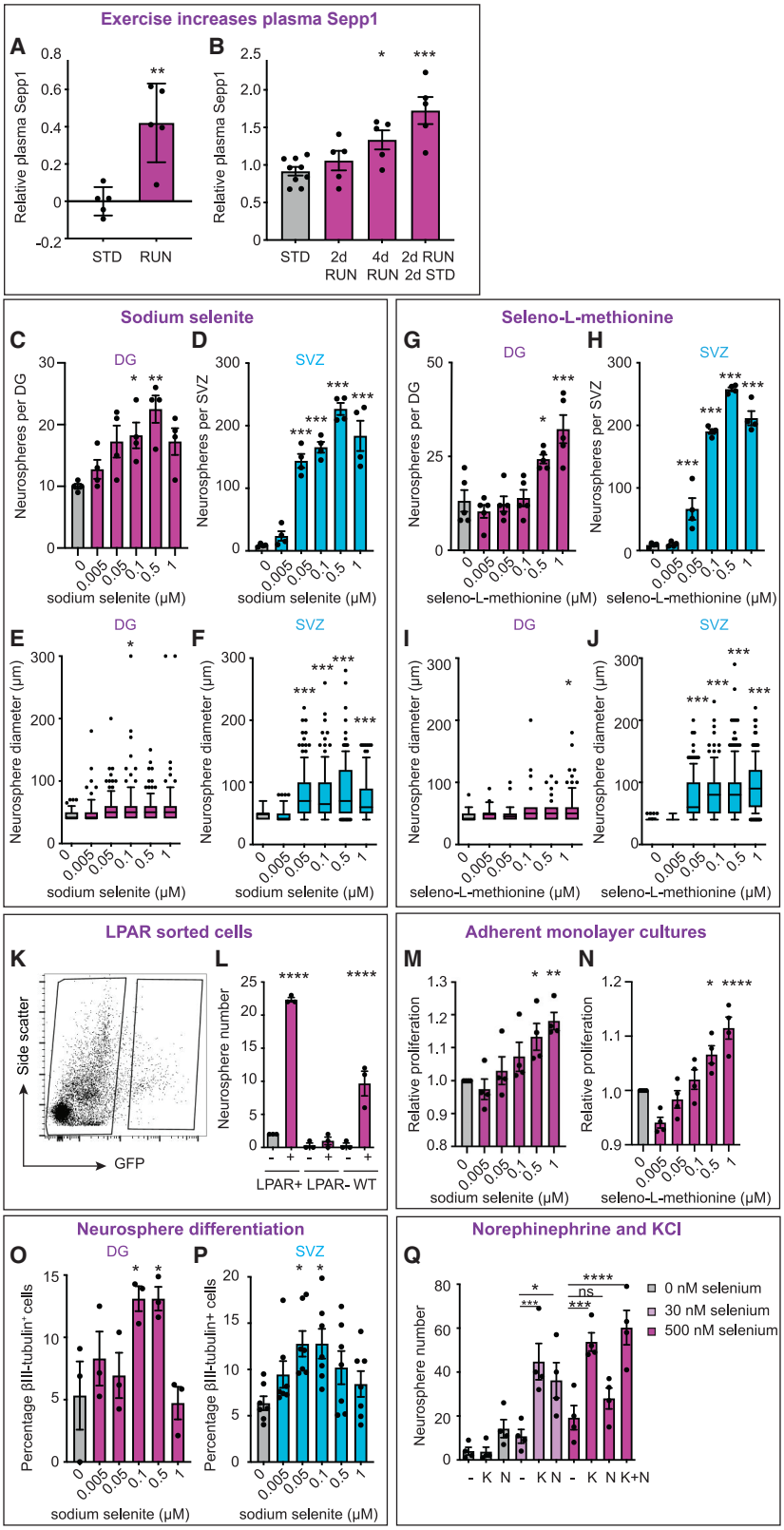

Figure 1. Selenium acts directly on NPCs *ex vivo*

(A) A mass-spectrometry-based proteomic screen revealed that selenoprotein P (Sepp1) is the most significantly upregulated protein in the plasma of mice after 4 days of wheel running.

(B) A significant increase in plasma Sepp1 levels after 4 days of exercise was confirmed using ELISA.

(C) Primary DG cells formed significantly more neurospheres when cultured in medium containing either 0.1 or 0.5 μM sodium selenite compared with medium devoid of selenium.

(D) Primary SVZ cells formed significantly more neurospheres when cultured in medium containing between 0.05 and 1 μM sodium selenite compared with medium devoid of selenium.

(E–J) The addition of selenium resulted in a significant increase in the average DG (E) and SVZ (F) neurosphere diameter. Primary DG and SVZ cells both formed more (G and H) and larger (I and J) neurospheres when cultured in medium containing increasing concentrations of seleno-L-methionine compared with medium devoid of selenium.

(K and L) LPA_1-GFP^+ cells responded directly to selenium treatment in the absence of other niche cells.

(M and N) Hippocampal adherent monolayer cultures displayed significantly increased proliferation following treatment with either sodium selenite (M) or seleno-L-methionine (N).

(O) Hippocampal neurospheres generated in the presence of 0.1 or 0.5 μM sodium selenite generated significantly more βIII-tubulin$^+$ neurons following differentiation.

(P) Similarly, sodium selenite increased the neuronal differentiation potential of SVZ-derived neurospheres.

(Q) Sodium selenite treatment activated the latent norepinephrine (N)-responsive, but not the KCl (K)-responsive stem cell population.

One-way ANOVA with Dunnett's post hoc test (B–D, G, H, and M–P) or Tukey's post hoc test (L and Q), Student's t test (A). *$p < 0.05$, **$p < 0.01$, ***$p < 0.001$, and ****$p < 0.0001$.

neurospheres generated. When primary DG cells were cultured in high levels of sodium selenite, the addition of 15 mM KCl led to a further significant increase in the neurosphere number (Figure 1Q). In contrast, treatment with 10 μM norepinephrine in addition to high selenium resulted in no further increase in the neurosphere number, suggesting that norepinephrine and selenium are activating the same population of precursor cells.

Selenium induces NPC proliferation and neurogenesis *in vivo*

Having shown that selenium increases NPC numbers *ex vivo*, we next sought to determine whether the same effect could be observed *in vivo*. To investigate this, we infused sodium selenite (1 μM) directly into the hippocampus for 7 days using micro-osmotic pumps and labeled the proliferating cells with the thymidine analog BrdU, 2 h prior to perfusion (Figure 2A). We found that selenium treatment resulted in a greater than 3-fold increase in the number of proliferating cells in the subgranular zone of the DG (Figure 2B). In contrast, selenium had no effect on the number of proliferating cells in the SVZ (Figure 2C). To confirm this effect, we performed a second experiment using the same infusion paradigm but with a lower dose of sodium selenite (200 nM). Again, selenium infusion significantly increased the number of proliferating precursor cells in the DG (Figure 2D) with no difference observed in the SVZ proliferation (Figure 2E). To confirm that the DG-specific effect was not due to the location of the cannula, we also infused 200 nM sodium selenite directly into the lateral ventricle (Figure 2F). Strikingly, this resulted in a significant increase in the number of proliferating precursor cells in the DG (Figure 2G), but not the SVZ (Figure 2H), confirming that selenium has a specific *in vivo* effect only on the precursor cells of the DG. Finally, we also quantified the number of activated caspase-3$^+$ cells in the DG of the selenium- and saline-infused mice. This revealed that, although apoptosis did occur, infusion of sodium selenite (200 nM) into the DG for 7 days had no effect on the total number of apoptotic (activated caspase3$^+$) cells *in vivo* (Figure S1C).

To determine whether selenium infusion could, in addition to increasing the number of proliferating precursor cells, increase net neurogenesis, we next labeled proliferating cells with the thymidine analog 5-chloro-2′-deoxyuridine (CldU) then infused sodium selenite (200 nM) into the DG for 28 days (Figure 2I). We found that selenium treatment resulted in a significant increase in net hippocampal neurogenesis *in vivo*, with more new neurons (CldU$^+$NeuN$^+$) surviving 4 weeks after the start of selenium infusion (Figure 2J). The number of proliferating (Ki67$^+$) cells remained increased at the end of the 28-day infusion period (Figure 2K). Similar to its effects on proliferation, 28 days of selenium infusion did not alter net neurogenesis levels in the olfactory bulb to which the SVZ projects via the rostral migratory stream (Figure 2L). We also investigated whether selenium treatment was required for the entire 28-day period in order to produce an increase in newborn neurons. In this experiment, sodium selenite (200 nM) was infused for 7 days, followed by a 3-week chase period (Figure 2M). The cells that were proliferating prior to the onset of selenium treatment were labeled with CldU on day 1, immediately after surgery, and the pool of proliferating cells that had expanded in response to 7 days of selenium treatment was labeled on day 8 using a second thymidine analog, 5-iodo-2′-deoxyuridine (IdU). We found that selenium treatment resulted in approximately 50% more surviving CldU$^+$ cells 3 weeks after the end of this treatment (Figure 2N). Phenotyping of these cells revealed that the majority of the newborn cells had differentiated into NeuN$^+$ neurons (Figure 2O). Short-term selenium infusion, therefore, resulted in an approximately 55% net increase in neurogenesis (Figure 2P). The data from the short-term infusion (Figure 2B) show that 7 days of selenium infusion increased the number of proliferating NPCs by approximately 300%. In this experiment, we found that labeling this already expanded NPC population with IdU after 7 days of selenium treatment, followed by a 3-week chase period during which the labeled cells could undergo additional divisions before becoming post-mitotic, resulted in a greater than 6-fold increase in the number of surviving IdU$^+$ cells (Figure 2Q). Together these results indicate that, in addition to its effect on the number of proliferating cells, selenium exerts an additional effect on newborn neuron survival.

Selenium preferentially recruits quiescent NPCs *in vivo*

There are several cellular mechanisms that could potentially explain the selenium-mediated increase in neurogenesis. These include increased survival of proliferating cells, cell-cycle shortening, increased number of cell divisions, or recruitment of quiescent stem cells (Overall et al., 2016). We have previously shown that the alteration of the cell-cycle length is not sufficient to explain the increased number of proliferating precursor cells observed after exercise (Fischer et al., 2014). We and others have instead proposed that physical activity increases the number of proliferating precursors by recruiting quiescent, activatable stem cells into proliferation (Adusumilli et al., 2021; Lugert et al., 2010). To determine whether acute selenium treatment causes an increase in proliferation by increasing the survival of the already dividing cells or by recruiting quiescent cells, we used a dual thymidine analog (CldU and IdU) labeling paradigm and a single intraperitoneal injection of selenium (Figure 2R). We found no difference in the percentage of either CldU$^+$IdU$^-$ cells (cells that were already proliferating prior to the selenium injection but had exited the cell cycle prior to the first IdU injection 24 h later) or CldU$^+$IdU$^+$ cells (cells that were already proliferating prior to the selenium injection and remained proliferative 24 h later when IdU was injected; Figure 2S). We did, however, observe a significant increase in the percentage of CldU$^-$IdU$^+$ cells (representing the cells that were non-dividing prior to the selenium treatment and entered proliferation during the 24-h selenium treatment time window; Figures 2S and 2T). To determine the identity of these CldU$^-$IdU$^+$ cells recruited by selenium treatment, we phenotyped them using two sets of antibodies to identify early progenitors (CldU/IdU/Sox2/Tbr2) and late progenitors (CldU/IdU/Tbr2/DCX). Our results revealed that the majority of the CldU$^-$IdU$^+$ cells were early progenitors that were either Sox2$^+$Tbr2$^-$, Sox2$^+$Tbr2$^+$, or Sox2$^-$Tbr2$^+$ (Figures 2U and 2V). Selenium treatment did not significantly alter the proportion of cells within these classes. Together, these findings suggest that selenium treatment, similar to physical activity, increases proliferation through the recruitment of quiescent cells into the neurogenic trajectory.

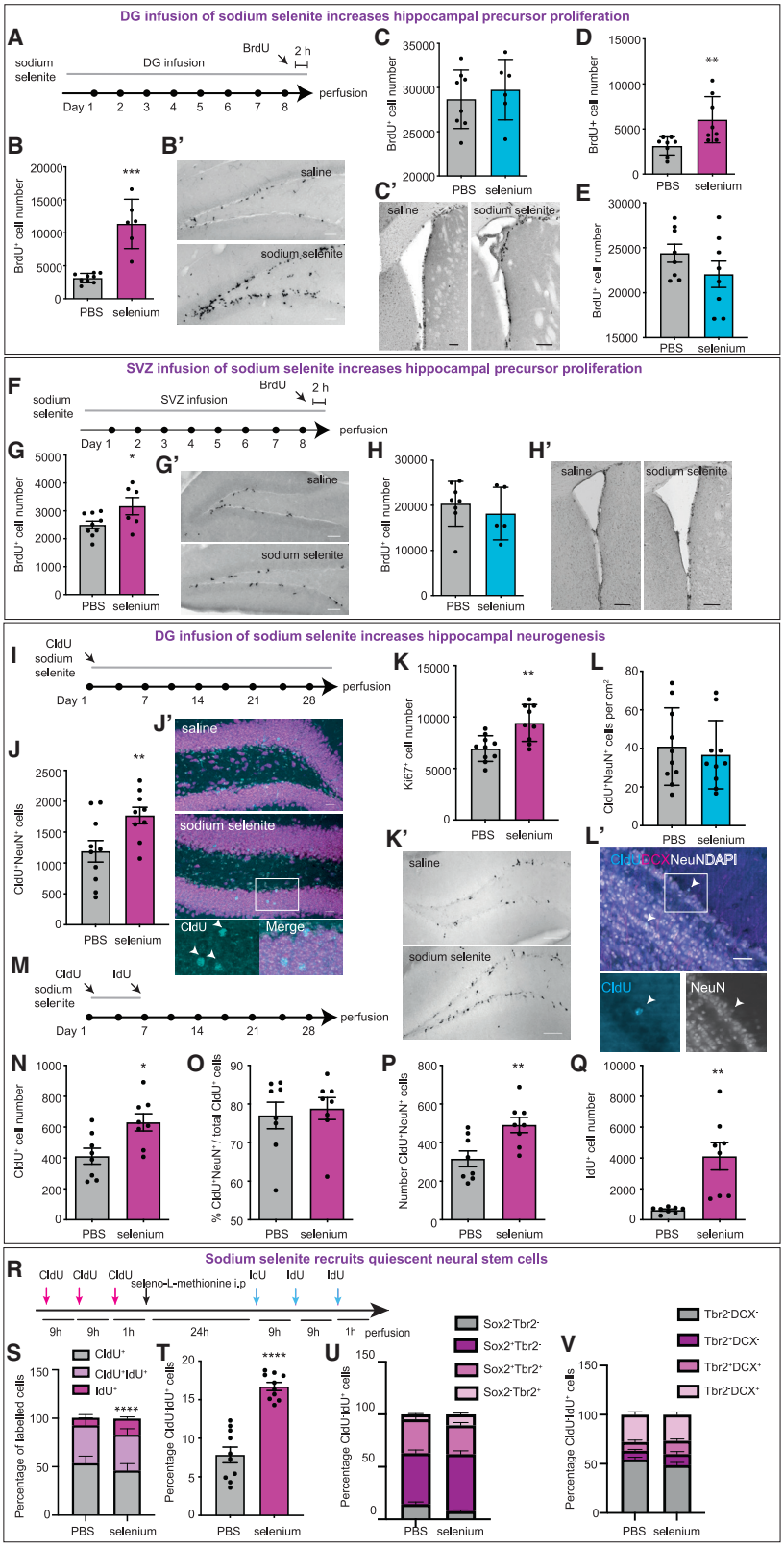

Figure 2. Selenium recruits quiescent NPCs *in vivo*

(A–E) Infusion of 1 μM sodium selenite into the DG for 7 days resulted in a greater than 3-fold increase in the number of $BrdU^+$ cells in the DG (A and B), but not the SVZ (C). When a lower concentration of sodium selenite (200 nM) was infused into the DG for 7 days a similar increase in proliferation was observed in the DG (D), but not in the SVZ (E).

(F–H) Infusion of 200 nM sodium selenite into the SVZ for 7 days resulted in a significant increase in the number of $BrdU^+$ cells in the DG (F and G) but had no effect on the number of proliferating cells in the SVZ (H).

(I and J) Infusion of 200 nM sodium selenite into the DG for 28 days resulted in a significant increase in the number of $CldU^+/NeuN^+$ newborn neurons in the DG.

(K) Proliferation ($Ki67^+$ cells) was also significantly increased by sodium selenite following 28 days of infusion.

(L) In contrast, infusion of 200 nM sodium selenite into the DG for 28 days had no effect on the number of $CldU^+/NeuN^+$ newborn neurons in the olfactory bulb.

(M–Q) A 7-day infusion of sodium selenite (200 nM) followed by a 3-week chase period resulted in a significant increase in the number of surviving newborn cells ($CldU^+$ cells) (M and N). The majority of the $CldU^+$ cells were $NeuN^+$ neurons (O). Although selenium treatment did not alter the percentage of newborn neurons, it significantly increased their total number (P). There was a significant increase in the number IdU-labeled cells following a 3-week post-selenium chase period (Q).

(R) Experimental paradigm for the dual thymidine labeling of proliferating cells.

(S and T) Intraperitoneal injection of 2 μg/g of seleno-L-methionine led to a significant increase in the percentage of cells ($CldU^-IdU^+$) recruited into the neurogenic trajectory.

(U and V) Phenotyping revealed that the majority of the $CldU^-IdU^+$ cells were early progenitors.

Two-way ANOVA with Šidák's post hoc test (S, U, and V) or Student's t test (all other panels). *$p < 0.05$, **$p < 0.01$, ***$p < 0.001$, and ****$p < 0.0001$. Scale bars, 100 μm. Arrowheads indicate $CldU^+$ cells in higher powered images in (J′) and (L′).

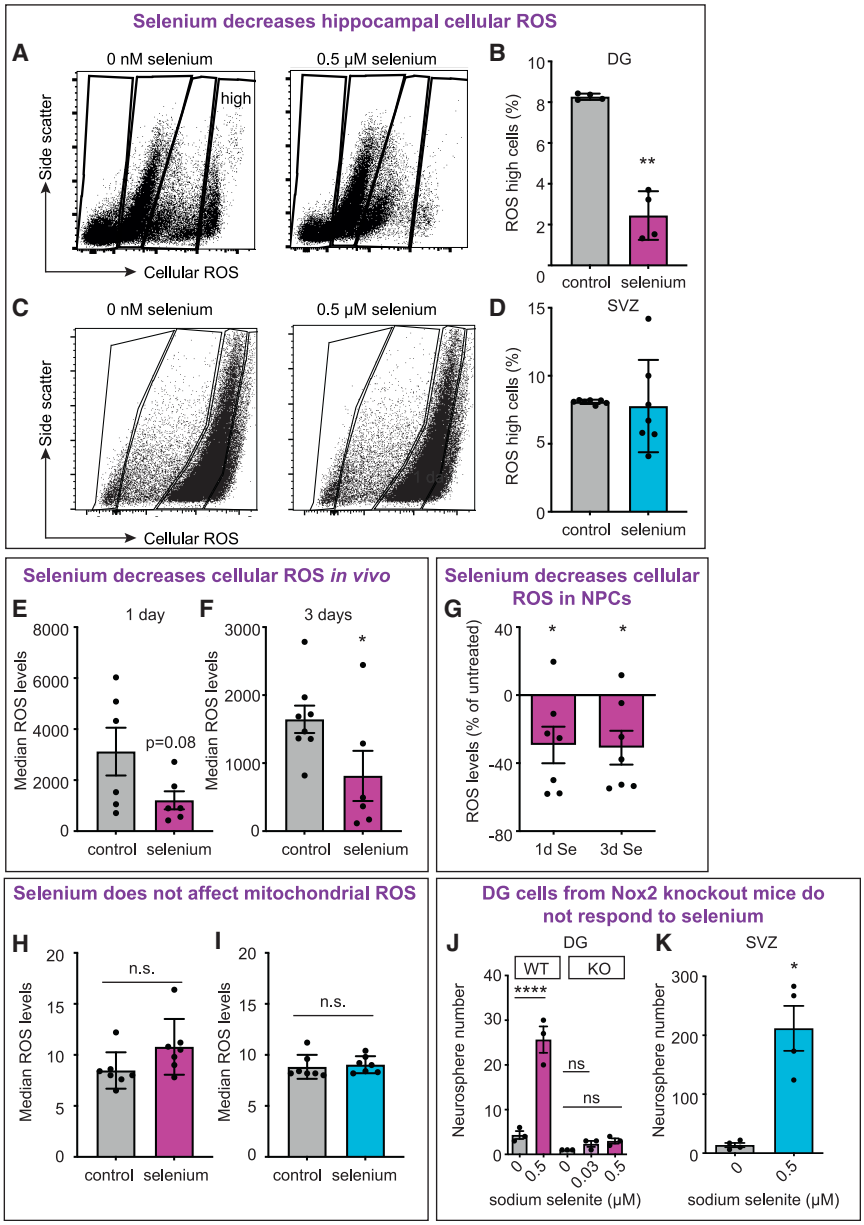

Figure 3. Selenium decreases cellular ROS

(A and B) The number of cells in the DG with high levels of intracellular ROS was decreased following treatment with 0.5 μM sodium selenite *ex vivo*.

(C and D) In contrast, the number of cells in the SVZ with high levels of intracellular ROS was unchanged following treatment with 0.5 μM sodium selenite.

(E and F) Infusion of sodium selenite into the DG for 1 day (E) or 3 days (F) decreased the median ROS levels.

(G–I) Treatment of cultures of adherent hippocampal NPCs with sodium selenite for 1 or 3 days significantly decreased the levels of cellular ROS (G). Sodium selenite treatment did not affect the levels of mitochondrial ROS in primary cells isolated from the DG (H) or SVZ (I).

(J) Primary DG-derived cells from Nox2$^{-/-}$ mice did not respond to selenium treatment.

(K) In contrast, SVZ precursor cells from Nox2$^{-/-}$ mice formed significantly more neurospheres when grown in selenium-supplemented medium.

One-way ANOVA with Dunnett post hoc test (G), one-way ANOVA with Tukey's post hoc test (J), and Student's t test (all other panels). *$p < 0.05$, **$p < 0.01$, and ****$p < 0.0001$.

Selenium decreases intracellular ROS levels in the hippocampal neurogenic niche

We have previously shown that fluctuations in the levels of intracellular reactive oxygen species (ROS) precede the exercise-induced activation of quiescent NPCs (Adusumilli et al., 2021). Having found that SEPP1 levels are significantly increased in the blood following exercise, and given that selenium and selenoproteins are known antioxidants, we next investigated whether selenium could reduce the levels of intracellular ROS in our cells. To investigate this, primary DG cells were treated with 0.5 μM sodium selenite for 16 h, after which intracellular ROS levels were measured by flow cytometry. The gates were set based on cells cultured without selenium, with the top approximately 8% of cells being designated as "ROS high" (Figure 3A). We found that treatment with 0.5 μM sodium selenite significantly reduced the number of DG cells in the high ROS fraction (Figure 3B). Notably, the ROS reduction appeared to be specific for the ROS high cells (and to a lesser extent to those with medium ROS levels), which we have recently shown to be primarily NPCs (Adusumilli et al., 2021). In contrast, treatment of primary SVZ-derived cells with sodium selenite had no effect on the distribution of the cells among the ROS classes (Figures 3C and 3D). To determine whether *in vivo* selenium treatment also led to decreases in cellular ROS in the DG, we infused selenium directly into the hippocampus for 3 days using mini osmotic pumps, after which we dissected the DG and directly determined the median ROS content of these primary cells. Importantly, we again observed a decrease in intracellular ROS following 1 and

3 days of selenium infusion (Figures 3E and 3F). To confirm that selenium supplementation could reduce the levels of intracellular ROS specifically in the precursor cell population, we turned to the adherent monolayer culture system, which consists of a near pure population of these cells. We found that following either 1 or 3 days of selenium treatment *in vitro*, adherent hippocampal precursor cells had significantly lower levels of intracellular ROS than untreated cells (Figure 3G). Although mitochondrial respiration is a major source of cellular ROS (Zorov et al., 2014), we have previously shown that exercise does not affect mitochondrial ROS levels in these cells (Adusumilli et al., 2021). Similarly, we observed no significant effect of selenium treatment on mitochondrial ROS levels (Figures 3H and 3I), indicating that the selenium-mediated ROS changes are due to changes in cellular, not mitochondrial ROS.

The selenium-induced activation of NPCs is Nox2-dependent

NADPH oxidase (Nox) enzymes are the major source of cellular ROS in many tissues, including the neurogenic regions of the brain (Le Belle et al., 2011; Nayernia et al., 2017). We have previously demonstrated that although Nox2 activity is not required to maintain baseline levels of adult neurogenesis, cell-autonomous Nox2-dependent ROS changes are required for the exercise-induced activation of quiescent neural stem cells and the subsequent increase in their proliferation (Adusumilli et al., 2021). To determine whether the selenium-induced changes in intracellular ROS were dependent on Nox2 activity, neurosphere assays were performed on primary DG or SVZ cells isolated from $Nox2^{-/-}$ mice and cultured in a medium containing either 0, 0.03, or 0.5 μM selenium. Similar to our previous results in wild-type mice, significantly more neurospheres were generated in SVZ-derived precursor cell cultures of $Nox2^{-/-}$ mice treated with 0.5 μM selenium (Figure 3K). In contrast, the DG-derived precursor cells of the Nox2 mutant mice did not respond to selenium treatment (Figure 3J), indicating that selenium-induced NPC activation in the DG is Nox2-dependent.

Sepp1-Lrp8-mediated selenium transport is required for the exercise-induced increase in NPC proliferation

Having determined that selenium increases neurogenesis specifically in the DG through the recruitment of quiescent neural stem cells, we next sought to identify the mechanism by which peripheral selenium enters the brain. Although there are 25 known selenoproteins, SEPP1 is of particular interest in the context of adult neurogenesis as it is required to transport selenium across the blood-brain barrier by binding to its receptor LRP8 on brain capillary endothelial cells. In mice, *Sepp1* deletion leads to a large decrease in brain selenium levels, but only a moderate decrease in most other tissues, confirming that SEPP1 is essential for adequate brain selenium supply (Hill et al., 2003). In addition, both *Sepp1* and *Lrp8* knockout mice develop severe neurodegeneration when exposed to selenium-deficiency levels that are tolerated by wild-type mice (Burk et al., 2014). In addition to its function at the blood-brain barrier, SEPP1-LRP8-mediated selenium transport is also important within the brain for the transport of selenium into cell populations. We first examined whether *Sepp1* is expressed to the same extent in the two neurogenic niches. Our results revealed that primary SVZ-derived cells had an over 2-fold higher expression of the *Sepp1* transcript than the primary cells of the DG (Figure 4A), suggesting that SVZ precursor cells partially depend on the baseline selenium provided by SEPP1 and potentially explaining why these cells do not respond to exogenously supplied selenium. In line with this explanation, we found that primary SVZ cells had significantly lower levels of *Lrp8* expression than those of the DG (Figure 4B), strengthening our conclusion that the NPCs of the SVZ are less responsive to selenium fluctuations. Using the neurosphere assay, we then investigated whether *Sepp1* depletion affected the responsiveness of the NPCs to exogenous selenium. As expected, the primary DG cells isolated from wild-type littermate brains were activated by selenium, leading to a significant increase in the number of neurospheres (Figure 4C). Although the effect size was much smaller, the primary DG cells of *Sepp1* knockout mice were also responsive to selenium activation (Figure 4D). No difference in the size of the neurospheres generated from *Sepp1* wild-type or knockout mice was observed (Figure 4E).

To investigate whether effective selenium transport to the brain is required to regulate the exercise-induced increase in hippocampal neurogenesis, we gave *Sepp1* and *Lrp8* knockout mice and their wild-type littermates access to running wheels for 7 days and compared them with standard-housed mice. Although they ran similar distances per night (Figure 4F), 10 days of wheel running did not increase NPC proliferation in the *Sepp1* knockouts as it did in their wild-type littermates (Figure 4G). However, we observed no difference in baseline proliferation (Figure 4H) or the levels of neurogenesis (Figure 4I) in the hippocampus of *Sepp1*-deficient mice. Phenotyping of the proliferating $Ki67^{+}$ cells in the *Sepp1* knockout and wild-type hippocampus revealed that most of these cells were $Sox2^{+}Tbr2^{+}$, $Sox2^{+}Tbr2^{-}$, or $Sox2^{-}Tbr2^{+}$ NPCs, with less than 3% of the proliferating cells being negative for both markers (Figure 4H). The relative proportion of the cells expressing each of the marker combinations was not changed by either genotype or exercise. *Lrp8* knockout mice also ran a similar distance to their wild-type littermates (Figure 4J). However, in contrast to the *Sepp1*-deficient mice, *Lrp8* knockout mice had a significant reduction in baseline proliferation (Figure 4K) and neurogenesis (Figure 4M). Similar to the *Sepp1*-null mice, the *Lrp8* knockout mice did not respond to the running stimulus (Figure 4K) and phenotyping of the proliferating cells revealed that neither genotype nor exercise changed the relative proportion of NPCs within each group of mice (Figure 4L). Together, these data support the idea that, in the hippocampus, effective selenium transport is particularly required for the activity-dependent increase in the precursor cell number.

Selenium compensates for the age-related reduction in neurogenesis and associated decrease in cognitive function

The results presented earlier demonstrate that selenium increases neurogenesis in the young adult (8- to 10-week-old) hippocampus. However, neural precursor proliferation and neurogenesis decrease significantly with age (Kuhn et al., 1996), concomitant with a decline in associated learning and memory function (Gil-Mohapel et al., 2013). It has previously been shown that the age-related decrease in plasma selenium levels

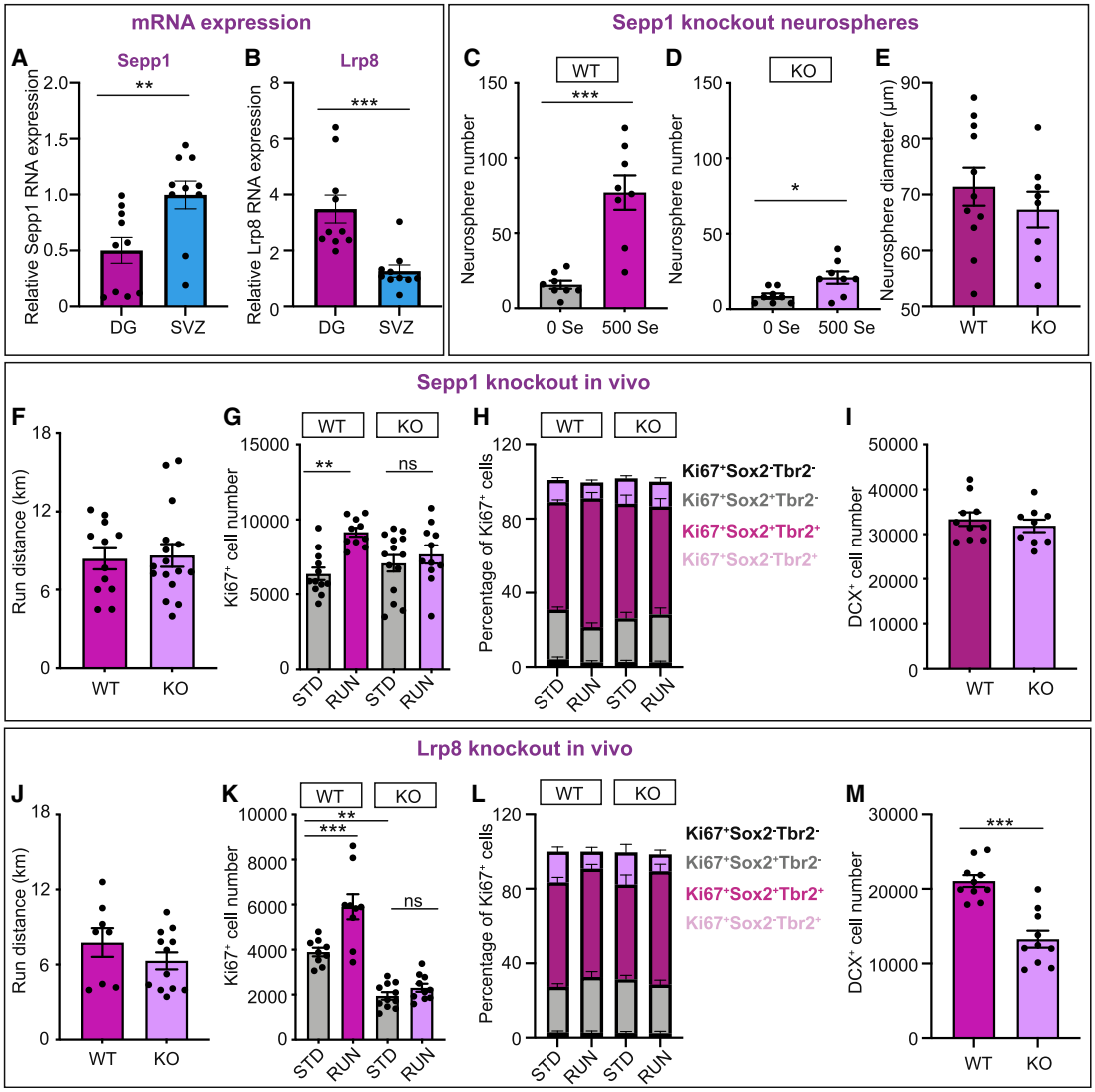

Figure 4. Sepp1-Lrp8-mediated selenium transport is required for the exercise-induced increase in NPC proliferation

(A) Expression of the *Sepp1* transcript was significantly lower in primary cells of the DG compared with the SVZ.

(B) In contrast, significantly higher levels of *Lrp8* expression were observed in the DG compared with the SVZ.

(C and D) Primary DG cells isolated from both wild-type (C) and Sepp1$^{-/-}$ (D) mice could be activated by selenium treatment.

(E) No difference in neurosphere diameter between wild-type and *Sepp1*$^{-/-}$ mice was observed.

(F) *Sepp1* wild-type and knockout mice ran a similar number of kilometers per night.

(G) Although no deficit in baseline proliferation was observed, *Sepp1* knockout mice did not respond to 7 days of wheel running.

(H) Phenotyping of the Ki67^{+} cells revealed that most of the proliferating cells were either Sox2^{+}Tbr2^{-}, Sox2^{+}Tbr2^{+}, or Sox2^{-}Tbr2^{+} NPCs, the relative percentages of which were not altered by genotype or exercise.

(I) *Sepp1* deletion had no effect on the number of DCX^{+} newborn neurons.

(J) *Lrp8* wild-type and knockout mice ran a similar number of kilometers per night.

(K) *Lrp8* knockout mice had lower baseline proliferation levels and did not respond to the running stimulus.

(L) Phenotyping of the Ki67^{+} cells revealed that most of the proliferating cells were either Sox2^{+}Tbr2^{-}, Sox2^{+}Tbr2^{+}, or Sox2^{-}Tbr2^{+} NPCs, the relative percentages of which were not altered by genotype or exercise.

(M) *Lrp8* deletion significantly decreased the number of DCX^{+} newborn neurons.

Student's t test (A–F, I, J, and M) or one-way ANOVA with Tukey's post hoc test (G, H, K, and L), *p < 0.05, **p < 0.01, and ***p < 0.001.

in humans positively correlates with the probability of cognitive decline (Akbaraly et al., 2007). We, therefore, next investigated whether selenium could rescue the dramatic decrease in neurogenesis observed in old (12- and 18-month-old) mice.

In a series of pilot experiments, we first investigated various selenium sources, concentrations, and delivery routes to determine the optimal treatment paradigm. We found that unilateral infusion of sodium selenite into the DG of 12-month-old mice

for 7 days, followed by a 3-week chase period (Figure S2A), resulted in a significant increase in the number of proliferating NPCs (Figures S2B and S2C) and net adult neurogenesis (Figures S2B and S2D) in both the ipsilateral and contralateral hippocampi, with no difference observed between hemispheres. The oldest animals tested (18 months; Figure S2E) also exhibited a large increase in both the number of proliferating NPCs ($BrdU^+$ cells; 17-fold; Figures S2F and S2G) and later-stage neurogenesis (doublecortin-positive [DCX^+] cells; 5.4-fold; Figures S2H and S2I) following 28 days of sodium selenite infusion. Surprisingly, however, and in contrast to young animals, we observed signs of tissue damage in the ipsilateral hemisphere of the old sodium selenite-infused mice. This damage originated at the infusion site and spread toward the rostral (bregma+ 1.18 mm) and caudal (bregma− 2.92 mm) brain regions (Figures S2J–S2M). To address this, we tested an alternative selenium source, the organic selenium compound seleno-L-methionine, which is known to have a lower toxicity than sodium selenite (Ammar and Couri, 1981). Infusion of seleno-L-methionine for 28 days significantly increased the number of proliferating precursor cells in the DG (Figures S2N–S2P). However, although tissue damage was significantly reduced following seleno-L-methionine infusion, it was not eliminated (Figures S2Q–S2T).

Given the observed selenium toxicity to brain tissue, we next investigated whether dietary selenium supplementation was a less damaging and more effective delivery strategy to increase neurogenesis. We chose to deliver selenium at 50 nM (10 ppm) in the drinking water, which is well below the levels reported to result in no observed adverse effects in mice (Abdo, 1994). We first used inductively coupled plasma mass spectrometry (ICP-MS) to confirm that 28 days of 50 nM seleno-L-methionine delivery via the drinking water was sufficient to significantly raise the plasma and DG selenium levels in both young and aged mice (Figures 5A and 5B), without affecting the brain levels of any of the other elements measured (Figure S3). We then investigated whether dietary selenium supplementation was sufficient to rescue the age-related decline in proliferating precursor cells (Figure 5C). Our results revealed that 18-month-old selenium-treated mice had significantly more proliferating NPCs (Figures 5D and 5F) and DCX^+ immature neurons (Figure 5E) in the DG than control mice. Body weight was not adversely affected by the treatment, and no brain tissue damage was observed.

To determine the effect of selenium supplementation on hippocampus-dependent spatial learning and memory, 17-month-old mice were given either saline or seleno-L-methionine (50 nM) in their drinking water for 4 weeks (Figure 6A) and were then assessed using the active place avoidance (APA) task (Figure 6B). This test is well-suited to old animals and has been used previously in the context of adult hippocampal neurogenesis research (Vukovic et al., 2013; Willis et al., 2020). In this task, mice are placed on a rotating platform and tested for their ability to learn to avoid a stationary shock zone using visual cues as a reference. The mice were first pre-tested using the APA task to establish their baseline cognitive abilities (Figure S4A), after which they were divided into two cohorts with equivalent learning that received either saline or selenium in their drinking water. As a general measure of health status, body weight was monitored throughout the experiment, with no adverse weight loss being observed in the selenium-treated animals (Figure S4B). In addition, no difference was observed in the volume of water consumed by the two groups. Following treatment, we found that, although there was no difference in the total distance traveled (Figure S4C), the selenium-treated mice were significantly better than the control mice at avoiding the shock zone, with fewer shocks received (Figures 6C–6E) and a greater time to both first (Figures 6F and 6G) and second (Figures 6H and 6I) entrance into this zone observed at day 4.

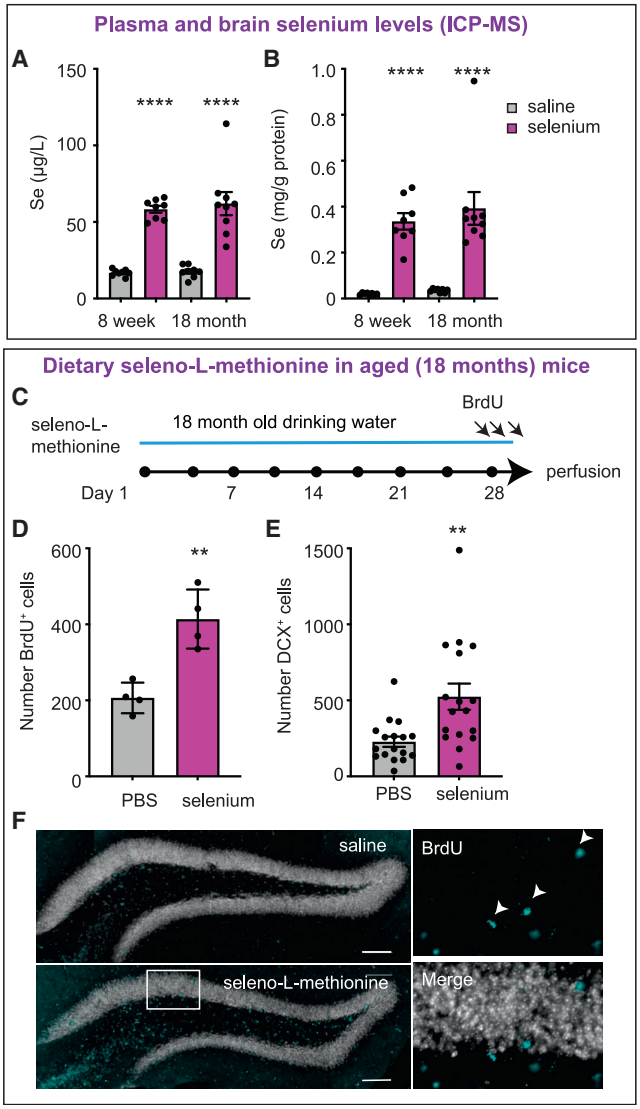

Figure 5. Dietary selenium compensates for the age-related reduction in neurogenesis

(A and B) ICP-MS analysis revealed a significant increase in plasma (A) and DG (B) selenium levels of both 8-week-old and 18-month-old mice following 4 weeks of dietary seleno-L-methionine supplementation.

(C) Schematic of the experimental protocol for delivery of seleno-L-methionine (50 nM) in the drinking water of 17-month-old mice for 28 days.

(D–F) Delivery of dietary seleno-L-methionine resulted in a significant increase in the number of proliferating precursor cells (D and F) and immature neurons (E) in the DG.

Student's t test. $^{**}p < 0.01$, $^{****}p < 0.0001$. Scale bars, 100 µm. Arrowheads indicate $BrdU^+$ cells in higher magnification images.

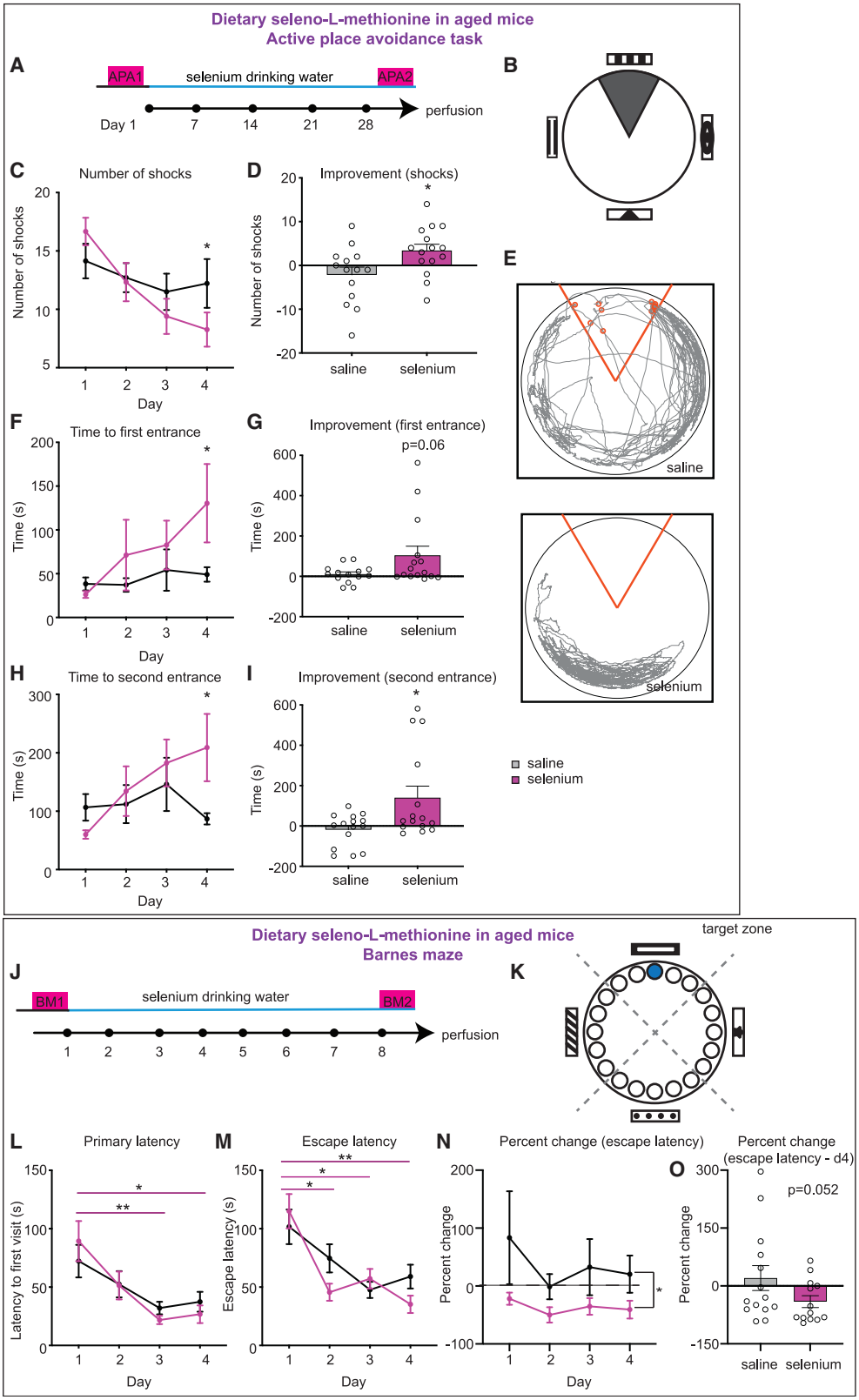

Figure 6. Dietary selenium supplementation rescues the age-related decline in hippocampus-associated learning and memory

(A and B) Experimental design for the active place avoidance (APA) test. Prior to selenium treatment, mice were pre-tested using the APA task and then divided into two cohorts with equivalent learning.

(legend continued on next page)

We corroborated these results using a second spatial learning task, the Barnes maze. In this task, the mice were placed in the center of a brightly lit table with 32 evenly spaced holes around its circumference (Figure 6K). The mice were tested for their ability to use the visual cues placed around the room to locate the one hole with an escape chamber located beneath it. As in the APA task, 16-month-old mice were pre-tested for their baseline learning ability using the Barnes maze and divided into two cohorts of equal learning ability (Figure S4D). The mice then received either saline or selenium in their drinking water for 8 weeks after which they were re-tested (Figure 6J). No effect of the selenium treatment on body weight (Figure S4E) or velocity (Figure S4F) was observed. Similar to the APA task, we found that selenium treatment significantly improved Barnes maze performance. Although there was no significant difference between the selenium-treated and control mice in the primary latency to the goal box or the escape latency, a Šidák post hoc analysis revealed that only the selenium-treated mice showed a significant decrease in their primary latency to the goal location on days 3 and 4 compared with those on day 1 (Figure 6L). In contrast, the primary latency of the control mice was not significantly improved over the 4-day testing period. The selenium-treated mice also learned to enter the escape box faster than the control mice (Figure 6M). Whereas the control mice displayed no significant improvement in the escape latency over the 4-day testing period, the selenium-treated mice entered the escape box significantly faster on days 2, 3, and 4 compared with those on the first day (Figure 6M). Further analysis comparing the post-treatment learning with pre-treatment learning revealed an overall significant positive effect of selenium on escape latency (Figures 6N and 6O). Together, these findings indicate that selenium supplementation can restore age-related deficits in hippocampal function.

Selenium rescues the hippocampal learning and memory deficits induced by an endothelin-1-induced hippocampal lesion

Unilateral stereotaxic injection of the vasoconstrictor endothelin-1 (ET-1) into the hippocampal fissure results in a stroke-like lesion that manifests as a significant reduction in the number of DCX^+ immature neurons and a decline in cognitive function that can be rescued by physical exercise (Codd et al., 2020). To investigate whether dietary selenium supplementation provides similar beneficial effects in this ischemic injury model to those observed with physiological aging, mice were first pre-tested using the APA task 5 weeks prior to ET-1 lesion to determine their baseline learning ability (Figure 7A). All animals showed a progressive decrease in the number of shocks received as they learned over the 5 days of testing (Figure S5A). The animals were subsequently evenly divided into 6 groups based on this performance and subjected to two additional APA tests (Figure 7A). Mice that received sham surgery performed significantly better than lesioned mice 3 days and 5 weeks after surgery (Figure S5A). We found that dietary seleno-L-methionine supplementation, either 4 weeks pre-treatment or beginning immediately following the lesion, exhibited no adverse effects on overall health (Figure S5B) and exploratory behavior measured using the open-field test (Figures S5F–S5H) but could completely rescue the spatial learning and memory deficits observed in the APA task 3 days (Figures 7B and 7C) and 5 weeks (Figures S5C–S5E) post-lesion.

Given that the ET-1-induced hippocampal lesion leads to a significant loss of DCX^+ newborn neurons, we next examined DG-dependent behavioral pattern separation using the novel object location (NOL) task (Figure 7D). On the habituation day, all six groups of mice spent a similar amount of time exploring the two objects (Figure S6D). Twenty-four hours later, on the test day, the ET-1-lesioned mice receiving standard drinking water spent significantly less time exploring the object presented in a novel location compared with sham mice (Figure 7E), whereas the mice receiving selenium-supplemented water, either immediately after the lesion or for the previous 4 weeks, performed as well as the controls (Figure 7E). There was no difference in the overall exploratory time of the mice between groups on the test day (Figure S6E). This result suggests that selenium treatment rescued the ET-1-induced behavioral pattern separation deficit. In a separate cohort of mice, following the same selenium treatment and ET-1-induced hippocampal lesion, we tested performance in the Y-maze, novel object recognition (NOR) test, and contextual fear conditioning test to evaluate spatial exploration behavior, long-term recognition, and contextual memory, respectively (Figure 7F). The NOR test was performed to assess recognition memory in mice based on their inherent preference for novelty (Figure 7G). In line with the results of the NOL test, all six groups of mice spent a similar amount of time exploring the two objects on the habituation day (Figure S6F). However, on the test day, ET-1-lesioned mice spent significantly less time exploring the object in a novel location compared with sham mice, suggesting an impairment in long-term recognition memory due to the lesion (Figure 7H). Selenium treatment, starting 4 weeks prior to the lesion, successfully rescued this deficit (Figure 7H). Following the NOR test, mice were assessed using contextual fear conditioning consisting of an 8-min exposure to a novel environment, with 1 s, 0.8 mA foot shocks delivered at 2, 4, 6, and 8 min (Figure 7I). Mice from all six groups exhibited similar acquisition of conditioned fear (Figure S6H). However, significantly less freezing was observed in ET-1-lesioned mice receiving standard drinking water compared with sham mice during the recall test 24 h after fear conditioning (Figure 7J), revealing an impairment in long-term contextual memory. This deficit could be rescued by selenium supplementation, with the lesioned mice receiving the selenium-supplemented water

(C–I) The selenium-treated mice performed significantly better at the APA task than control mice, with fewer shocks (C–E), and a greater time to both first (F and G) and second (H and I) entrance into the shock zone observed at day 4.

(J–N) Experimental design for the Barnes maze test (J and K). Selenium treatment significantly improved Barnes maze performance, decreasing primary latency to the goal location (L) and escape latency (M). A significant positive effect of selenium treatment on the percentage improvement in escape latency between the pre-treatment and post-treatment learning was observed (N).

Two-way repeated measures (RM) ANOVA with Šidák post hoc test (C, F, H, L, and M) and two-way RM ANOVA (N) (selenium effect $F(1,25) = 5.05$; $p = 0.03$). *$p < 0.05$, **$p < 0.01$.

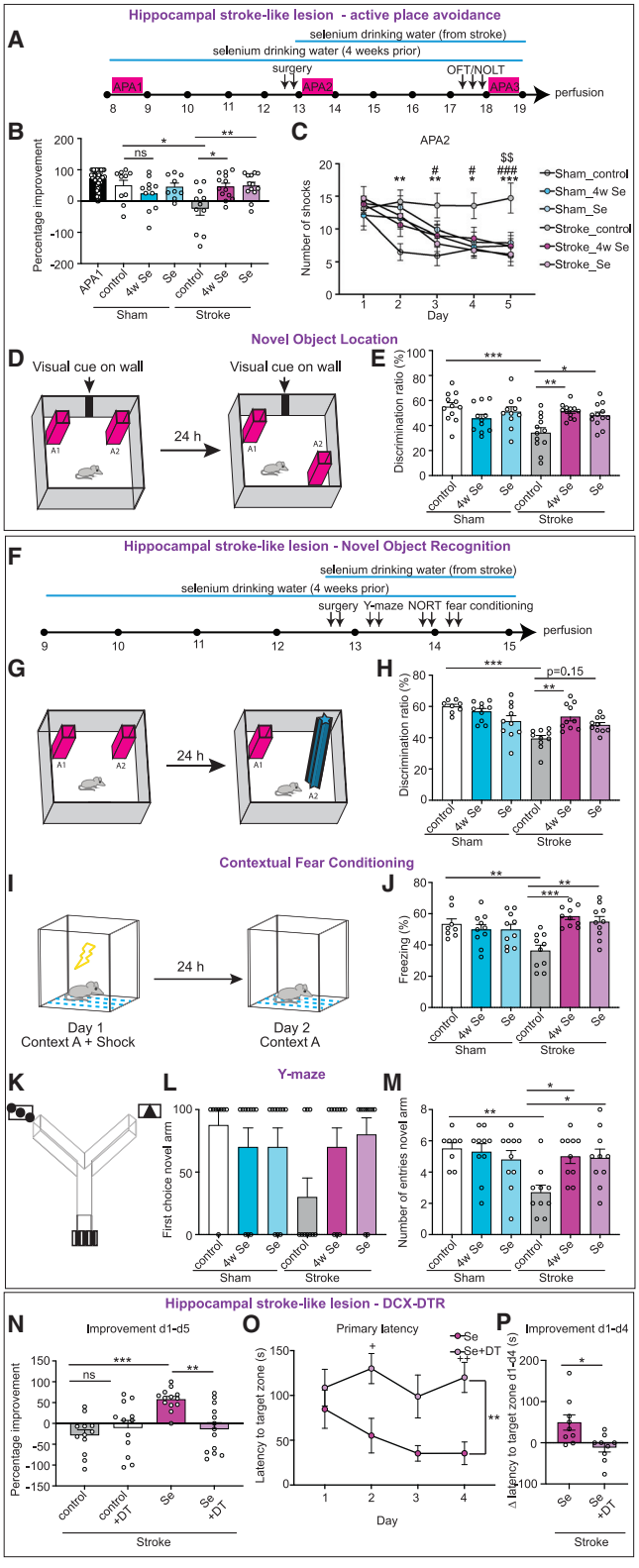

Figure 7. Selenium rescues the hippocampal learning and memory deficit induced by an endothelin-1-induced hippocampal lesion

(A) Experimental design.

(B and C) Improvement in the APA 2 test, expressed as (B) percentage improvement, and (C) mean number of shocks. *sham_control versus lesion_control; #lesion_control versus lesion_Se; $lesion_control versus lesion_4w Se.

(D) Schematic illustrating the novel object location test paradigm.

(E) The percentage of exploration time spent on the object in a novel location in the test session, expressed as a discrimination ratio.

(F) Experimental design.

(G) Schematic illustrating the novel object recognition test paradigm.

(H) The percentage of exploration time spent on the novel object in the test session, expressed as a discrimination ratio.

(I) Schematic illustrating the contextual fear conditioning paradigm.

(J) Freezing behavior in the fear recall test.

(K) Schematic illustrating the Y-maze paradigm.

(L) Selenium-treated, lesioned mice preferentially entered the novel arm first compared with lesioned mice receiving control drinking water.

(M) Selenium-treated, lesioned mice made significantly more entries to the novel arm than lesioned mice receiving control drinking water.

(N) The number of shocks received by DCX-DTR mice in the APA 2 test, expressed as the percentage improvement between day 1 and 5.

(O) Primary latency to the goal location in the Barnes maze over the 4 testing days.

(P) The improvement from day 1 to 4 in latency to the target zone (in seconds).

One-way ANOVA with Bonferroni post hoc test (B, E, H, J, M, and N), two-way repeated measures ANOVA with Bonferroni post hoc test (C), and logistic regression analysis (L). *$p < 0.05$, **$p < 0.01$, and ***$p < 0.001$. Two-way repeated measures ANOVA (effect of DT treatment $F(1,16) = 9.353$; $p = 0.008$) with Šidák post hoc test +$p < 0.05$, ++$p < 0.01$ (O).

exhibiting significantly more freezing than the lesioned mice that received standard water (Figure 7J). Finally, spatial exploration was examined using the Y-maze task. In this task, mice with good spatial memory should be able to remember the arm that they visited in the habituation session and be more inclined to visit the novel arm in the test session (Figure 7K). Although there was no difference in the total distance traveled during the test (Figure S6I), the majority of the mice receiving the selenium-supplemented drinking water entered the novel arm first (Figure 7L), entered the novel arm significantly more times (Figure 7M), and spent a significantly higher percentage of time in the novel arm during the first 60 s (Figure S6J) than the lesioned mice receiving the standard drinking water. Taken together, these results show that selenium treatment, either 4 weeks prior to or immediately after an ET-1-induced hippocampal lesion, successfully ameliorated the associated cognitive deficits.

Finally, to determine whether the effect of selenium in this model is adult neurogenesis-dependent, we used a transgenic knockin DCX^{DTR} mouse strain, which we developed to specifically delete cells at the DCX^{+} stages of adult neurogenesis (Vukovic et al., 2013). DCX^{DTR} mice express the human diphtheria toxin receptor (DTR) on the surface of DCX^{+} cells, which can be selectively ablated by treatment with DT, with the resident DCX^{-} NPCs remaining intact. DCX^{DTR} mice were pre-tested in the APA test 11 days prior to lesion to determine their baseline cognitive ability. All mice received a unilateral ET-1-induced hippocampal lesion and were then treated with either seleno-L-methionine water or control water and injected with DT or saline for 2 weeks (Figure S6K). A second APA task revealed that the ablation of DCX^{+} newborn neurons blocked the beneficial effect of the selenium treatment (Figures 7N and S6L). Quantification of DCX^{+} cells confirmed that the ET-1-induced lesion resulted in a significant reduction in DCX^{+} newborn neurons (Figures S6M

and S6N). We confirmed the results mentioned earlier in a separate experiment in which mice were treated as described earlier but were assessed using the Barnes maze. We again found that DT-induced ablation of DCX$^+$ newborn cells markedly reduced the learning capacity of selenium-treated, ET-1-lesioned mice, as evidenced by a significant reduction in primary latency to the goal location (Figures 7O and 7P). Together, these results indicate that, here, selenium is functioning in a neurogenesis-dependent manner.

DISCUSSION

Although the neurogenesis-enhancing effects of exercise have been known for more than two decades (van Praag et al., 1999a, 1999b), the molecular mechanisms underlying this response have remained largely unclear. Taken together, our data show that an exercise-induced increase in antioxidant selenium transport activates quiescent hippocampal NPCs, resulting in increased NPC proliferation and adult neurogenesis. Furthermore, we show that mimicking the exercise-induced increase in systemic selenium transport by dietary selenium supplementation can restore neurogenesis and reverse the cognitive decline associated with aging and hippocampal injury.

The hippocampal NPC niche is highly vascularized, allowing for direct contact between the circulatory system and the NPCs. Studies using heterochronic parabiosis, in which the circulatory systems of young and old mice are connected, were the first to suggest the involvement of the systemic environment as a central mediator of adult hippocampal neurogenesis and physiological brain aging (Villeda et al., 2011, 2014). More recently, systemic blood factors have been shown to transfer the beneficial effects of exercise to the aged hippocampus (Horowitz et al., 2020). In their plasma proteomic screen, Horowitz et al. did not identify SEPP1 as being increased in the blood following exercise. Interestingly, however, another selenoprotein, glutathione peroxidase 3, was identified as one of the most significantly upregulated proteins. This difference is likely due to differences in the age of the mice and the running paradigms used (6 weeks of running in aged mice in the Horowitz study compared with 4 days of running in young mice in our study).

In further support of the systemic mediation of adult hippocampal neurogenesis, basement membrane-reduced zones located between radial glial-like processes of the hippocampal NPCs and endothelial cells have recently been discovered (Licht et al., 2020), revealing a communication route that allows for direct access between the systemic environment and the NPCs of the DG. Our results suggest that exercise increases the transport of selenium from the systemic environment to NPCs of the DG by elevating the systemic level of SEPP1, which binds to LRP8 expressed on endothelial cells. Interestingly, a similar route of access between the systemic environment and the other major neurogenic region of the brain, the SVZ, does not seem to exist (Licht et al., 2020). We propose that this finding provides an explanation for why blood components that are known to be changed by exercise exclusively affect hippocampal neurogenesis without influencing proliferation in the SVZ. Fitting with this hypothesis, we found that similar to exercise, *in vivo* selenium supplementation increased hippocampal but not SVZ NPC proliferation.

In addition to differential exposure to the systemic environment, another factor contributing to the contrasting response of the two NPC populations to exercise is their unique transcriptional signatures (Adusumilli et al., 2021). In contrast to the NPCs of the SVZ, where the most enriched gene ontology pathways are related to cell division and transcriptional regulation, the most highly enriched pathway in the DG is redox regulation, with the NPCs of the DG being maintained in a more highly oxidized state than those of the SVZ (Adusumilli et al., 2021). We have identified redox regulation as the critical mediator of the exercise-dependent recruitment of quiescent hippocampal NPCs into the proliferative state (Adusumilli et al., 2021). We subsequently identified the antioxidant SEPP1 as one of the most significantly increased systemic proteins released in response to exercise (Leiter et al., 2019). In this study, we found that exogenous selenium treatment lowers cellular ROS levels in both primary cells of the DG niche and pure populations of adherent hippocampal NPCs and triggers the recruitment of quiescent hippocampal NPCs into the neurogenic trajectory *in vivo*. Fitting with this finding and highlighting the key role of SEPP1 in this process, we also observed that transgenic SEPP1 or LRP8 deletion abolishes the exercise-induced increase in NPC proliferation. We, therefore, propose that exercise-induced SEPP1 release contributes to our previously identified ROS-mediated mechanism of exercise-induced activation of quiescent NPCs. In contrast to the DG, we found that, under baseline conditions, primary SVZ cells had an over 2-fold higher expression level of *Sepp1* and significantly lower levels of *Lrp8* transcript than the primary cells of the DG. We speculate that the lower cellular ROS content, mediated by higher basal levels of antioxidant SEPP1, may explain why the SVZ precursor cells do not respond to exogenously supplied selenium (or exercise).

An interesting facet of this issue is the presence of multiple subpopulations of non-dividing hippocampal NPCs that are responsive to different stimuli (Jhaveri et al., 2015; Walker et al., 2008). In this study, we found that selenium activates the same population of quiescent NPCs as norepinephrine, further characterizing this quiescent NPC population. Our finding that selenium transport mediates the exercise-induced NPC activation, therefore, identified the norepinephrine-responsive population as the one that is activated in response to exercise. This is in agreement with the earlier finding that GABA, a known inhibitor of NPC activation and exercise-induced neurogenesis (Dumitru et al., 2017), selectively inhibits the activation of the norepinephrine-responsive but not the KCl-responsive subpopulation of hippocampal NPCs (Jhaveri et al., 2015).

Selenium is important for maintaining normal brain function and its deficiency has been linked to a number of age-related neurodegenerative disorders, including Alzheimer's disease, Parkinson's disease, and Huntington's disease (Cardoso et al., 2015). Selenium status also declines naturally with age (Akbaraly et al., 2007). In this study, we showed that selenium supplementation can rescue the decreased hippocampal neurogenesis and associated learning and memory deficits in animal models of physiological aging and ET-1-induced hippocampal lesion, models in which the cognitive deficits have also been shown to be rescued by physical exercise (Codd et al., 2020; Horowitz

et al., 2020). It has been reported that, during aging, increased quiescence rather than stem cell depletion accounts for the observed decrease in neurogenesis (Kalamakis et al., 2019; Lugert et al., 2010). In support of this, we found that although NPC proliferation was greatly reduced in the aged hippocampus, the magnitude of selenium-induced activation was greater in older mice than young mice. This is similar to our previous observation in aged mice following KCl-induced hippocampal NPC activation (Walker et al., 2008). Determining whether long-term activation of quiescent NPCs by selenium supplementation (or exercise) results in their depletion or whether these NPCs divide asymmetrically to continually self-renew following selenium-induced activation will provide insight into the life-long maintenance of NPC populations in the DG.

Overall, our finding that selenium metabolism is involved in mediating the exercise-induced increase in adult hippocampal neurogenesis demonstrates how systemic or environmental factors can regulate adult neurogenesis and hence plasticity in the DG. This could have far-reaching implications, as the activity-dependency of adult hippocampal neurogenesis is one of its key features and central to modern concepts of how adult-generated neurons provide life-long adaptability to the hippocampus in both health and disease. The identification of the mechanism underlying the exercise-induced increase in adult neurogenesis could facilitate the discovery of novel therapeutic interventions (including dietary selenium supplementation), which could be used to mimic the beneficial effects of exercise on cognitive function. Given that selenium is a cheap, readily available dietary supplement that is found in a number of commonly eaten foods, such as nuts, grains, and dairy products, it could easily be boosted in the diet of elderly people. This is particularly important for the treatment of individuals who are unable to exercise due to advanced age, frailty, or disability.

Limitations of study

In this study, we have identified systemic SEPP1 as a mediator of the exercise-induced proliferation of quiescent hippocampal NPCs. However, the source of the released SEPP1 remains unknown. Although the liver is the major source of plasma SEPP1, lower levels of *Sepp1* mRNA are also expressed in other tissues(-Hill et al., 2012). Transgenic mice in which SEPP1 is specifically deleted in hepatocytes could be used to resolve this issue. Furthermore, several additional systemic regulators of the exercise-induced increase in neurogenesis have already been described, pointing to a multi-factorial route of activation. These include cathepsin B (Moon et al., 2016), platelet factor 4 (Leiter et al., 2019), brain-derived neurotrophic factor (Farmer et al., 2004), vascular endothelial growth factor (Fabel et al., 2003), insulin-like growth factor 1 (Trejo et al., 2001), and Gpld1 (Horowitz et al., 2020). How these factors work synergistically, what their individual contributions are, and whether they affect the same population of cells as SEPP1 remain to be determined.

STAR★METHODS

Detailed methods are provided in the online version of this paper and include the following:

- KEY RESOURCES TABLE
- RESOURCE AVAILABILITY
  - Lead contact
  - Materials availability
  - Data and code availability
- EXPERIMENTAL MODEL AND SUBJECT DETAILS
  - Mice
- METHOD DETAILS
  - Neurosphere culture
  - Adherent monolayer cultures
  - Resazurin assay
  - Immunostaining of neurospheres
  - *In vivo* infusions
  - Intracellular ROS measurements
  - MitoSOX measurements
  - BrdU and Ki67 immunohistochemistry and quantification of proliferation
  - CldU and NeuN fluorescence immunohistochemistry and quantification of neuronal survival
  - BrdU and NeuN fluorescence immunohistochemistry and quantification of neuronal survival in aged animals
  - CldU and IdU fluorescence immunohistochemistry
  - Quantitative real-time PCR
  - Inductively coupled plasma-mass spectrometry
  - Hippocampal lesion surgery
  - Running distance tracking
  - Behavioral testing
  - Active place avoidance test
  - Barnes maze
  - Open field test
  - Novel object recognition test
  - Novel object location test
  - Contextual fear conditioning
  - Y-maze
- QUANTIFICATION AND STATISTICAL ANALYSIS

SUPPLEMENTAL INFORMATION

Supplemental information can be found online at https://doi.org/10.1016/j.cmet.2022.01.005.

ACKNOWLEDGMENTS

This work was funded by the Brazil Family Foundation for Neurology, Australia; the Deutsche Forschungsgemeinschaft SFB 655; and the Clem Jones Centre for Ageing Dementia Research. We thank Anne Karasinsky and Sandra Günther for care and maintenance of animals and Rowan Tweedale for her helpful comments on the manuscript. Z.Z. was supported by a SUSTech-UQ Joint Graduate Student Scholarship. S.-T.H. was supported by grants from the National Natural Science Foundation of China (81871026) and the Shenzhen-Hong Kong Institute of Brain Science-Shenzhen Fundamental Research Institutions (2019SHIBS0002 and 2021SHIBS0002).

AUTHOR CONTRIBUTIONS

Experimentation, O.L., Z.Z., T.L.W., R.R., L.G., J.M.W., S.K., D.B., V.S.A., D.G.B., N.R., A.M.S., A.E.R., A.S., S.A., K.G., and S.Z.; analysis, R.W.O. and A.S.; manuscript preparation, T.L.W., R.W.O., and G.K.; supervision, T.L.W., P.F.B., G.K., A.I.B., S.A., C.A.M., and S.-T.H.; funding acquisition, T.L.W., G.K., and S.-T.H. All authors reviewed the manuscript.

DECLARATION OF INTERESTS

The authors declare no competing interests.

Received: May 4, 2021
Revised: October 1, 2021
Accepted: January 11, 2022
Published: February 3, 2022

REFERENCES

Abdo, K.M. (1994). National toxicity program technical report on toxicity studies of sodium selenate and sodium selenite. National Toxicity Program Toxicity Report Series *38*, 1–127.

Adusumilli, V.S., Walker, T.L., Overall, R.W., Klatt, G.M., Zeidan, S.A., Zocher, S., Kirova, D.G., Ntitsias, K., Fischer, T.J., Sykes, A.M., et al. (2021). ROS dynamics delineate functional states of hippocampal neural stem cells and link to their activity-dependent exit from quiescence. Cell Stem Cell *28*, 300–314.e6.

Akbaraly, T.N., Hininger-Favier, I., Carrière, I., Arnaud, J., Gourlet, V., Roussel, A.M., and Berr, C. (2007). Plasma selenium over time and cognitive decline in the elderly. Epidemiology *18*, 52–58.

Ammar, E.M., and Couri, D. (1981). Acute toxicity of sodium selenite and selenomethionine in mice after ICV or IV administration. Neurotoxicology *2*, 383–386.

Boldrini, M., Fulmore, C.A., Tartt, A.N., Simeon, L.R., Pavlova, I., Poposka, V., Rosoklija, G.B., Stankov, A., Arango, V., Dwork, A.J., et al. (2018). Human hippocampal neurogenesis persists throughout aging. Cell Stem Cell *22*, 589–599.e5.

Brown, J., Cooper-Kuhn, C.M., Kempermann, G., Van Praag, H., Winkler, J., Gage, F.H., and Kuhn, H.G. (2003). Enriched environment and physical activity stimulate hippocampal but not olfactory bulb neurogenesis. Eur. J. Neurosci. *17*, 2042–2046.

Burk, R.F., Hill, K.E., Motley, A.K., Winfrey, V.P., Kurokawa, S., Mitchell, S.L., and Zhang, W. (2014). Selenoprotein P and apolipoprotein E receptor-2 interact at the blood-brain barrier and also within the brain to maintain an essential selenium pool that protects against neurodegeneration. FASEB J *28*, 3579–3588.

Cardoso, B.R., Roberts, B.R., Bush, A.I., and Hare, D.J. (2015). Selenium, selenoproteins and neurodegenerative diseases. Metallomics *7*, 1213–1228.

Codd, L.N., Blackmore, D.G., Vukovic, J., and Bartlett, P.F. (2020). Exercise reverses learning deficits induced by hippocampal injury by promoting neurogenesis. Sci. Rep. *10*, 19269.

Curzon, P., Rustay, N.R., and Browman, K.E. (2009). Cued and contextual fear conditioning for rodents. In Methods of Behavior Analysis in Neuroscience, J.J. Buccafusco, ed. (CRC Press), pp. 19–37.

Dumitru, I., Neitz, A., Alfonso, J., and Monyer, H. (2017). Diazepam binding inhibitor promotes stem cell expansion controlling environment-dependent neurogenesis. Neuron *94*, 125–137.e5.

Fabel, K., Fabel, K., Tam, B., Kaufer, D., Baiker, A., Simmons, N., Kuo, C.J., and Palmer, T.D. (2003). VEGF is necessary for exercise-induced adult hippocampal neurogenesis. Eur. J. Neurosci. *18*, 2803–2812.

Farmer, J., Zhao, X., van Praag, H., Wodtke, K., Gage, F.H., and Christie, B.R. (2004). Effects of voluntary exercise on synaptic plasticity and gene expression in the dentate gyrus of adult male Sprague-Dawley rats in vivo. Neuroscience *124*, 71–79.

Fischer, T.J., Walker, T.L., Overall, R.W., Brandt, M.D., and Kempermann, G. (2014). Acute effects of wheel running on adult hippocampal precursor cells in mice are not caused by changes in cell cycle length or S phase length. Front. Neurosci. *8*, 314.

Gil-Mohapel, J., Brocardo, P.S., Choquette, W., Gothard, R., Simpson, J.M., and Christie, B.R. (2013). Hippocampal neurogenesis levels predict water-maze search strategies in the aging brain. PLoS One *8*, e75125.

Gong, S., Zheng, C., Doughty, M.L., Losos, K., Didkovsky, N., Schambra, U.B., Nowak, N.J., Joyner, A., Leblanc, G., Hatten, M.E., and Heintz, N. (2003). A gene expression atlas of the central nervous system based on bacterial artificial chromosomes. Nature *425*, 917–925.

Hill, K.E., Wu, S., Motley, A.K., Stevenson, T.D., Winfrey, V.P., Capecchi, M.R., Atkins, J.F., and Burk, R.F. (2012). Production of selenoprotein P (Sepp1) by hepatocytes is central to selenium homeostasis. J. Biol. Chem. *287*, 40414–40424.

Hill, K.E., Zhou, J., Austin, L.M., Motley, A.K., Ham, A.J., Olson, G.E., Atkins, J.F., Gesteland, R.F., and Burk, R.F. (2007). The selenium-rich C-terminal domain of mouse selenoprotein P is necessary for the supply of selenium to brain and testis but not for the maintenance of whole body selenium. J. Biol. Chem. *282*, 10972–10980.

Hill, K.E., Zhou, J., McMahan, W.J., Motley, A.K., Atkins, J.F., Gesteland, R.F., and Burk, R.F. (2003). Deletion of selenoprotein P alters distribution of selenium in the mouse. J. Biol. Chem. *278*, 13640–13646.

Horowitz, A.M., Fan, X., Bieri, G., Smith, L.K., Sanchez-Diaz, C.I., Schroer, A.B., Gontier, G., Casaletto, K.B., Kramer, J.H., Williams, K.E., and Villeda, S.A. (2020). Blood factors transfer beneficial effects of exercise on neurogenesis and cognition to the aged brain. Science *369*, 167–173.

Jhaveri, D.J., Mackay, E.W., Hamlin, A.S., Marathe, S.V., Nandam, L.S., Vaidya, V.A., and Bartlett, P.F. (2010). Norepinephrine directly activates adult hippocampal precursors via beta3-adrenergic receptors. J. Neurosci. *30*, 2795–2806.

Jhaveri, D.J., O'Keeffe, I., Robinson, G.J., Zhao, Q.Y., Zhang, Z.H., Nink, V., Narayanan, R.K., Osborne, G.W., Wray, N.R., and Bartlett, P.F. (2015). Purification of neural precursor cells reveals the presence of distinct, stimulus-specific subpopulations of quiescent precursors in the adult mouse hippocampus. J. Neurosci. *35*, 8132–8144.

Kalamakis, G., Brüne, D., Ravichandran, S., Bolz, J., Fan, W., Ziebell, F., Stiehl, T., Catalá-Martinez, F., Kupke, J., Zhao, S., et al. (2019). Quiescence modulates stem cell maintenance and regenerative capacity in the aging brain. Cell *176*, 1407–1419.e14.

Kuhn, H.G., Dickinson-Anson, H., and Gage, F.H. (1996). Neurogenesis in the dentate gyrus of the adult rat: age-related decrease of neuronal progenitor proliferation. J. Neurosci. *16*, 2027–2033.

Kurokawa, S., Bellinger, F.P., Hill, K.E., Burk, R.F., and Berry, M.J. (2014). Isoform-specific binding of selenoprotein P to the b-propeller domain of apolipoprotein E receptor 2 mediates selenium supply. J. Biol. Chem. *289*, 9195–9207.

Le Belle, J.E., Orozco, N.M., Paucar, A.A., Saxe, J.P., Mottahedeh, J., Pyle, A.D., Wu, H., and Kornblum, H.I. (2011). Proliferative neural stem cells have high endogenous ROS levels that regulate self-renewal and neurogenesis in a PI3K/Akt-dependant manner. Cell Stem Cell *8*, 59–71.

Leiter, O., Seidemann, S., Overall, R.W., Ramasz, B., Rund, N., Schallenberg, S., Grinenko, T., Wielockx, B., Kempermann, G., and Walker, T.L. (2019). Exercise-induced activated platelets increase adult hippocampal precursor proliferation and promote neuronal differentiation. Stem Cell Rep *12*, 667–679.

Licht, T., Sasson, E., Bell, B., Grunewald, M., Kumar, S., Kreisel, T., Ben-Zvi, A., and Keshet, E. (2020). Hippocampal neural stem cells facilitate access from circulation via apical cytoplasmic processes. Elife *9*, e52134.

Lugert, S., Basak, O., Knuckles, P., Haussler, U., Fabel, K., Götz, M., Haas, C.A., Kempermann, G., Taylor, V., and Giachino, C. (2010). Quiescent and active hippocampal neural stem cells with distinct morphologies respond selectively to physiological and pathological stimuli and aging. Cell Stem Cell *6*, 445–456.

Massey, P.V., Warburton, E.C., Wynick, D., Brown, M.W., and Bashir, Z.I. (2003). Galanin regulates spatial memory but not visual recognition memory or synaptic plasticity in perirhinal cortex. Neuropharmacology *44*, 40–48.

Moon, H.Y., Becke, A., Berron, D., Becker, B., Sah, N., Benoni, G., Janke, E., Lubejko, S.T., Greig, N.H., Mattison, J.A., et al. (2016). Running-induced systemic cathepsin B secretion is associated with memory function. Cell Metab *24*, 332–340.

Moreno-Jiménez, E.P., Flor-García, M., Terreros-Roncal, J., Rábano, A., Cafini, F., Pallas-Bazarra, N., Ávila, J., and Llorens-Martín, M. (2019). Adult hippocampal neurogenesis is abundant in neurologically healthy subjects and drops sharply in patients with Alzheimer's disease. Nat. Med. *25*, 554–560.

Nayernia, Z., Colaianna, M., Robledinos-Antón, N., Gutzwiller, E., Sloan-Béna, F., Stathaki, E., Hibaoui, Y., Cuadrado, A., Hescheler, J., Stasia, M.-J., et al. (2017). Decreased neural precursor cell pool in NADPH oxidase 2-deficiency:

from mouse brain to neural differentiation of patient derived iPSC. Redox Biol *13*, 82–93.

Overall, R.W., Walker, T.L., Fischer, T.J., Brandt, M.D., and Kempermann, G. (2016). Different mechanisms must be considered to explain the increase in hippocampal neural precursor cell proliferation by physical activity. Front. Neurosci. *10*, 362.

Perez-Riverol, Y., Csordas, A., Bai, J., Bernal-Llinares, M., Hewapathirana, S., Kundu, D.J., Inuganti, A., Griss, J., Mayer, G., Eisenacher, M., et al. (2019). The PRIDE database and related tools and resources in 2019: improving support for quantification data. Nucleic Acids Res. *47*, D442–D450.

Pollock, J.D., Williams, D.A., Gifford, M.A., Li, L.L., Du, X., Fisherman, J., Orkin, S.H., Doerschuk, C.M., and Dinauer, M.C. (1995). Mouse model of X-linked chronic granulomatous disease, an inherited defect in phagocyte superoxide production. Nat. Genet. *9*, 202–209.

Reynolds, B.A., and Weiss, S. (1992). Generation of neurons and astrocytes from isolated cells of the adult mammalian central nervous system. Science *255*, 1707–1710.

Reynolds, B.A., Tetzlaff, W., and Weiss, S. (1992). A multipotent EGF-responsive striatal embryonic progenitor cell produces neurons and astrocytes. J. Neurosci. *12*, 4565–4574.

Spalding, K.L., Bergmann, O., Alkass, K., Bernard, S., Salehpour, M., Huttner, H.B., Boström, E., Westerlund, I., Vial, C., Buchholz, B.A., et al. (2013). Dynamics of hippocampal neurogenesis in adult humans. Cell *153*, 1219–1227.

Tobin, M.K., Musaraca, K., Disouky, A., Shetti, A., Bheri, A., Honer, W.G., Kim, N., Dawe, R.J., Bennett, D.A., Arfanakis, K., and Lazarov, O. (2019). Human hippocampal neurogenesis persists in aged adults and Alzheimer's disease patients. Cell Stem Cell *24*, 974–982.e3.

Trejo, J.L., Carro, E., and Torres-Aleman, I. (2001). Circulating insulin-like growth factor I mediates exercise-induced increases in the number of new neurons in the adult hippocampus. J. Neurosci. *21*, 1628–1634.

van Praag, H., Christie, B.R., Sejnowski, T.J., and Gage, F.H. (1999a). Running enhances neurogenesis, learning, and long-term potentiation in mice. Proc. Natl. Acad. Sci. USA *96*, 13427–13431.

van Praag, H., Kempermann, G., and Gage, F.H. (1999b). Running increases cell proliferation and neurogenesis in the adult mouse dentate gyrus. Nat. Neurosci. *2*, 266–270.

Villeda, S.A., Luo, J., Mosher, K.I., Zou, B., Britschgi, M., Bieri, G., Stan, T.M., Fainberg, N., Ding, Z., Eggel, A., et al. (2011). The ageing systemic milieu negatively regulates neurogenesis and cognitive function. Nature *477*, 90–94.

Villeda, S.A., Plambeck, K.E., Middeldorp, J., Castellano, J.M., Mosher, K.I., Luo, J., Smith, L.K., Bieri, G., Lin, K., Berdnik, D., et al. (2014). Young blood reverses age-related impairments in cognitive function and synaptic plasticity in mice. Nat. Med. *20*, 659–663.

Vukovic, J., Borlikova, G.G., Ruitenberg, M.J., Robinson, G.J., Sullivan, R.K., Walker, T.L., and Bartlett, P.F. (2013). Immature doublecortin-positive hippocampal neurons are important for learning but not for remembering. J. Neurosci. *33*, 6603–6613.

Walker, T.L., and Kempermann, G. (2014). One mouse, two cultures: isolation and culture of adult neural stem cells from the two neurogenic zones of individual mice. J. Vis. Exp. *(84):*, e51225.

Walker, T.L., White, A., Black, D.M., Wallace, R.H., Sah, P., and Bartlett, P.F. (2008). Latent stem and progenitor cells in the hippocampus are activated by neural excitation. J. Neurosci. *28*, 5240–5247.

Walker, T.L., Overall, R.W., Vogler, S., Sykes, A.M., Ruhwald, S., Lasse, D., Ichwan, M., Fabel, K., and Kempermann, G. (2016). Lysophosphatidic acid receptor is a functional marker of adult hippocampal precursor cells. Stem Cell Rep *6*, 552–565.

Willis, E.F., MacDonald, K.P.A., Nguyen, Q.H., Garrido, A.L., Gillespie, E.R., Harley, S.B.R., Bartlett, P.F., Schroder, W.A., Yates, A.G., Anthony, D.C., et al. (2020). Repopulating microglia promote brain repair in an IL-6-dependent manner. Cell *180*, 833–846.e16.

Yamaguchi, M., Saito, H., Suzuki, M., and Mori, K. (2000). Visualization of neurogenesis in the central nervous system using nestin promoter-GFP transgenic mice. Neuroreport *11*, 1991–1996.

Zorov, D.B., Juhaszova, M., and Sollott, S.J. (2014). Mitochondrial reactive oxygen species (ROS) and ROS-induced ROS release. Physiol. Rev. *94*, 909–950.

STAR★METHODS

KEY RESOURCES TABLE

REAGENT or RESOURCE	SOURCE	IDENTIFIER
Antibodies		
Mouse anti-β-III-tubulin (clone 5G8)	Promega	Cat# G7121; RRID: AB_430874
Mouse anti-BrdU (clone BMC9318)	Roche	Cat# 11170376001; RRID: AB_514483
Rat anti-BrdU (BrdU / CldU labelling; clone BU1/75)	Bio-Rad / AbD Serotec	Cat# OBT0030; RRID: AB_609568
Mouse anti-BrdU (IdU labelling; clone B44)	BD Biosciences	Cat# 347580; RRID: AB_10015219
Rabbit anti-cleaved caspase 3	Abcam	Cat# ab2302; RRID: AB_302962
Goat anti-DCX (polyclonal)	Santa Cruz	Cat# sc-8066; RRID: AB_2088494
Guinea pig anti-DCX	Millipore	Cat#AB2253; RRID: AB_1586992
Rabbit anti-GFAP (polyclonal)	Agilent/ Dako	Cat # Z0334; RRID: AB_10013382
Rat anti-Ki67 (clone SolA15)	eBioscience	Cat# 14-5698-82; RRID: AB_10854564
Rabbit anti-Tbr2	Abcam	Cat# ab183991; RRID: AB_2721040
Goat anti-Sox2	R&D Systems	Cat# AF2018; RRID: AB_355110
Rabbit anti-NeuN (polyclonal)	Abcam	Cat# ab104225; RRID: AB_10711153
Donkey anti-mouse Cy3	Jackson ImmunoResearch	Cat#715-165-151; RRID: AB_2315777
Donkey anti-rabbit Alexa Fluor 647	Jackson ImmunoResearch	Cat# 711-605-152; RRID: AB_2492288
Donkey anti-rabbit DyLight 488	Thermo Fisher Scientific	Cat# SA5-10038; RRID: AB_2556618
Donkey anti-rat biotin	Jackson ImmunoResearch	Cat# 712-065-153; RRID: AB_2315779
Donkey anti-rat Alexa Fluor 488	Jackson ImmunoResearch	Cat# 712-545-153; RRID: AB_2340684
Donkey anti-rat Alexa Fluor 594	Jackson ImmunoResearch	Cat# 712-585-153; RRID: AB_2340689
Goat anti-rat Alexa Fluor 488	Jackson ImmunoResearch	Cat#112-545-167; RRID: AB_2338362
Donkey anti-mouse Alexa Fluor 405	Abcam	Cat# ab175658; RRID: AB_2687445
Donkey anti-goat Alexa Fluor 488	Jackson ImmunoResearch	Cat# 705-545-147; RRID: AB_2336933
Donkey anti-mouse Alexa Fluor 568	Abcam	Cat# ab175472; RRID: AB_2636996
Goat anti-guinea pig Alexa Fluor 568	Invitrogen	Cat# A11075; RRID: AB_2534119
Goat anti-Rabbit Alexa Fluor 647	Thermo Fisher Scientific	Cat# A21245; RRID: AB_2535813
Chemicals, peptides, and recombinant proteins		
Apotransferrin	Sigma-Aldrich	Cat#T1147-100MG
Aqua Polymount	Polysciences	Cat# 18606-20
5-Bromo-2'deoxyuridine (BrdU)	Sigma-Aldrich	Cat# B5002
B27 supplement	Thermo Fisher Scientific	Cat# 17504044
Bovine serum albumin	Sigma-Aldrich	A8412-100ML
CellROX Deep Red reagent	Thermo Fisher Scientific	Cat# C10422
5-Chloro-2'deoxyuridine (CldU)	Sigma-Aldrich	Cat# C6891
DAPI	Invitrogen	Cat# D1306
Diaminobenzidine (DAB)	Sigma-Aldrich	Cat#D5905
DNaseI	Sigma-Aldrich	Cat# 4536282001
Endothelin-1	Sigma-Aldrich	Cat# E7764
Epidermal growth factor	Peprotech	Cat# AF-100-15
Basic fibroblast growth factor	Peprotech	Cat# AF-100-18B
Fluorescence mounting medium	Agilent /Dako	Cat# S302380-2
GlutaMAX supplement	Thermo Fisher Scientific	Cat# 35050061
Heparin	MP Biomedicals	Cat# 0210193125
5-Iodo-2'-deoxyuridine (IdU)	Sigma-Aldrich	Cat# I7125
Insulin	Sigma	Cat# I6634-50MG

(*Continued on next page*)

Continued

REAGENT or RESOURCE	SOURCE	IDENTIFIER
Neurobasal medium	Thermo Fisher Scientific	Cat# 21103049
L-(-)-noradrenaline(+)-bitartrate salt monohydrate	Merck	Cat# A9512
Laminin	Roche	Cat# 11243217001
MitoSOX Red mitochondrial superoxide indicator	Thermo Fisher Scientific	Cat# M36008
Neo-Clear	Merck	Cat# 109843
Neo-Mount	Merck	Cat# 109016
Propidium Iodide	Thermo Fisher Scientific	Cat# P3566
Poly-D-lysine (PDL)	Sigma-Aldrich	Cat# P7280
Progesterone	Sigma-Aldrich	Cat# P0130
Putrescine	Sigma-Aldrich	Cat# 51799
Potassium chloride	Sigma-Aldrich	Cat# P9333
Resazurin	Sigma-Aldrich	Cat# R7017
Sodium selenite	Sigma-Aldrich	Cat# 214485
Seleno-L-methionine	Sigma-Aldrich	Cat# S3132
0.05 % Trypsin-EDTA	Thermo Fisher Scientific	Cat# 25300054
Trypsin inhibitor	Sigma-Aldrich	Cat# 10109886001
Critical commercial assays		
Neural Tissue Dissociation Kit (P)	MACS Miltenyi Biotec	Cat# 130-092-628
VECTASTAIN Elite ABC-HRP Kit	Vector Laboratories	Cat# PK-6100
SEPP1/Selenoprotein P ELISA Kit	LifeSpan BioSciences	Cat# LS-F24254
Experimental models: Organisms/strains		
Mouse: LPA_1-GFP (Tg(Lpar1-EGFP) GX193Gsat/Mmucd)	Mutant Mouse Resource & Research Centre	Tg(Lpar1-EGFP)GX193Gsat/Mmucd
Mouse: C57BL/6JRj	Janvier Labs, France	Cat# SC-C57J-F
Mouse: B6.129-*Selenop*^{tm1Rfb}/J	The Jackson Laboratory	Cat# 008201
Mouse: B6;129S6-*Lrp8*^{tm1Her}/J	The Jackson Laboratory	Cat# #003524
Mouse: Nestin-GFP	(Yamaguchi et al., 2000)	N/A
Software and algorithms		
Freeze Frame	Actimetrics	version 4
Ethovision XT	Noldus	version XT14
Graph Pad Prism 6 for Mac OS X	N/A	version 6.0f
FlowJo	BD Bioscience	v10
Other		
Osmotic pumps (7d)	Alzet	Cat# 1007D
Osmotic pumps (28d)	Alzet	Cat# 1004

RESOURCE AVAILABILITY

Lead contact

Further information and requests for resources and reagents should be directed to and will be fulfilled by the lead contact, Dr. Tara Walker (t.walker1@uq.edu.au).

Materials availability

This study did not generate new unique reagents.

Data and code availability

- The mass spectrometry proteomics data have been deposited to the ProteomeXchange Consortium via the PRIDE (Perez-Riverol et al., 2019) partner repository with the dataset identifier PXD027324. All values used to generate the graphs of the paper can be found in the file Data S1.

- This study did not generate any code.
- Any additional information required to reanalyze the data reported in this paper. Is available from the lead contact upon request.

EXPERIMENTAL MODEL AND SUBJECT DETAILS

Mice

Mice were maintained on a 12/12 h light/dark cycle at between 21-22 °C and housed in pairs with access to standard mouse chow (in Dresden: Ssniff R/M-H; catalogue # V1534 and in Brisbane: Specialty Feeds, young mice catalogue # SF00-100 and aged mice catalogue # SF00-105) and autoclaved water *ad libitum* and inspected daily by responsible animal caretakers at either the Centre for Regenerative Technologies Dresden or the University of Queensland. All animals were 8 weeks old at the time of the experiment, unless otherwise stated. C57BL/6JRj mice were purchased from Janvier Labs as required, LPA_1-GFP mice (Tg(Lpar1-EGFP) GX193Gsat/Mmucd; (Gong et al., 2003; Walker et al., 2016) were purchased from the Mutant Mouse Resource & Research Centre and maintained as a hemizygous breeding colony. Nox2 knockout mice (B6.129S-Cybb^{tm1Din}/J; Pollock et al., 1995) were initially purchased from The Jackson Laboratory and maintained as a heterozygous breeding colony. *Sepp1* knockout mice (B6.129-*Selenop*^{tm1Rfb}/J) were purchased from The Jackson Laboratory and maintained as a heterozygous breeding colony, *Lrp8* knockout mice (B6;129S6-*Lrp8*^{tm1Her}/J) were purchased from The Jackson Laboratory and maintained as a heterozygous breeding colony, DCX^{DTR} mice were previously generated in our laboratory and were maintained as a homozygous breeding colony (Vukovic et al., 2013). All transgenic mice were maintained on a C57BL/6J background and wildtype littermates were used for all experiments involving the *Sepp1*, *Lrp8* and *Nox2* lines. All C57BL6/J mice were female and transgenic mice were mixed sex. All experiments were conducted in accordance with the applicable European or Australian regulations and approved by the responsible authority (Landesdirektion Sachsen or the University of Queensland Animal Ethics Committee).

METHOD DETAILS

Neurosphere culture

8 week-old C57BL/6 mice were killed and their brain was immediately removed. The DG and SVZ were microdissected as described previously (Walker and Kempermann, 2014). Briefly, the brain was placed on its ventral surface and bisected along the longitudinal fissure then rotated dorsal side up and cut coronally at the level of the optic chiasm. To dissect the SVZ, the rostral portion of the brain was placed with the cut side upwards and the septum removed. The SVZ was then dissected by cutting the approximately 1 mm of tissue adjacent to the ventricle with a pair of curved forceps. To dissect the DG, the cerebellum and diencephalon were removed from the caudal portion of the brain and a 27-gauge needle was used to cut along the border of the DG. The SVZ tissue was dissociated by mincing the tissue with a scalpel and transferring to a tube containing 1 ml of 0.05% Trypsin-EDTA and incubating for 7 min at 37°C. The enzymatic reaction was stopped by adding an equal volume of trypsin inhibitor containing DNaseI and centrifugation at 300 x g for 5 mins. The DG tissue was enzymatically digested using the Neural Tissue Dissociation Kit (P) (Miltenyi) according to the manufacturer's instructions. Following a final wash in Hank's balanced salt solution (HBSS) (PAA; GE Healthcare) the pellet was resuspended in 1 ml of growth medium and filtered through a 40 μm cell sieve (Falcon; BD Biosciences). Given that commercially purchased hormone supplements contain sodium selenite, we customised a hormone mix as described by Reynolds and colleagues (Reynolds et al., 1992). The culture medium consisted of insulin (25 μg/ml), apotransferrin (100 μg/ml), progesterone (20 nM), putrescine (60 μM), glucose (0.6 %), sodium bicarbonate (3 mM), HEPES (5 mM), bovine serum albumin (2 %), Penacillin/ streptomycin (50 U/ml), Heparin (2 μg/ml), basic fibroblast growth factor (20 ng/ml) and epidermal growth factor (20 ng/ml) in DMEM/F12. The DG and SVZ cells were diluted to a final volume of 20 ml in growth medium and plated into a 96-well plate. Cells were seeded into 96-well plates at a density of approximately 5 cells/μl for SVZ and 7.5 cells/μl for DG-derived cells, a density which has previously been shown to result in the formation of clonally derived neurospheres. Compounds were added to the growth medium at the time of plating and included sodium selenite (0.005–1 μM; Sigma-Aldrich), seleno-L-methionine (0.005 –1 μM; Sigma-Aldrich), KCl (15 mM; Sigma-Aldrich) or norepinephrine (L-(-)-noradrenaline(+)-bitartrate salt monohydrate; 10 μM; Merck). Plates were incubated for 7 d (SVZ) or 14 d (DG) at 37°C with 5% CO_2, and the resulting neurospheres were counted and sized using an inverted light microscope fitted with an ocular graticule.

For differentiation, neurospheres were plated onto poly-D-lysine (PDL; 10 μg/ml) and laminin (5 μg/ml)-coated coverslips in neurosphere growth medium without growth factors. The neurospheres were allowed to differentiate for 7 d in humidified 5 % CO_2 until flattened and adherent. The differentiated neurospheres were then fixed with 4 % paraformaldehyde (PFA; Sigma-Aldrich) in PBS at room temperature for 15 min.

Adherent monolayer cultures

To generate adherent monolayer cultures, primary DG cells from a single C57BL/6 mouse were plated into one well of a PDL- and laminin-coated 24-well plate in 1 ml of adherent culture growth medium. The growth medium consisted of Neurobasal A medium with 2 % B27 supplement, 1 % penicillin/streptomycin, 1 % Glutamax supplemented with basic fibroblast growth factor (20 ng/ml) and epidermal growth factor (20 ng/ml). The growth medium was changed every 2–3 d, and the cells were passaged when they reached approximately 80 % confluency.

Resazurin assay

Initially, a stock solution of 0.5 mM was prepared by dissolving resazurin dye (7-hydroxy-3H-phenoxazin-3-one 10-oxide) in dH_2O and subsequently sterile filtered. Approximately 10^4 cells/cm^2 passage 9–13 hippocampal adherent cells were plated on coated 24-well plates in proliferation medium. After 24 h, the medium was exchanged and supplemented with sodium selenite in a concentration range of 0 mM–1 μM. The cytotoxicity assay was performed after another 24 h. Resazurin solution was added (10 % of cell culture volume) to a final working concentration of 0.05 mM and the cells were incubated for 2 h at 37°C. Samples were analysed fluorometrically using a spectrophotometer (Infinite 7200; Tecan) by monitoring the emitted fluorescence signal at a wavelength of 590 nm when excited at 535 nm. Background signals obtained from cell-free wells were subtracted from each sample.

Immunostaining of neurospheres

The differentiated neurospheres were fixed with 4 % PFA in 0.1 M phosphate buffer at room temperature for 20 min. After washing with PBS, the cells were incubated in blocking solution (10 % normal donkey serum in PBS containing 0.2 % Triton X-100) for 60 min at room temperature. They were then incubated in fresh blocking solution containing mouse monoclonal βIII-tubulin antibody (1:1000; Promega) and rabbit GFAP antibody (1:500; Dako Cytomation) for 60 min at room temperature. The cells were washed three times with PBS and incubated in fresh blocking solution containing donkey anti-mouse Cy3 antibody (1:1000; Jackson ImmunoResearch), DyLight 488 donkey anti-rabbit antibody (1:1000; Dianova) and 4′,6-diamidino-2-phenylindole (DAPI; 1:5000; Sigma-Aldrich) for 30 min at room temperature. Following another three PBS washes, the slides were mounted using fluorescence mounting medium (Dako Cytomation) before being viewed at 20x magnification on a Zeiss Apotome microscope.

In vivo infusions

Micro-osmotic pumps (Alzet, #1004; 28 d infusion at a flow rate of 0.11 μl/h or Alzet, #1007; 7 d infusion at a flow rate of 0.5 μl/h) were loaded with sodium selenite (1 μM or 200 nM), or saline, and the cannula inserted to enable unilateral infusion directly into the hilus region of the hippocampus (anterior/posterior -1.3 mm, dorsal/lateral +1.0 mm, dorsal/ventral -2.2 mm, relative to Bregma) or SVZ (anterior/posterior +0.26 mm, dorsal/lateral +0.75 mm, dorsal/ventral -2.5 mm, relative to Bregma).

Intracellular ROS measurements

Adherent cultures

Adherent monolayer cells (passage 9–13) were plated into PDL/laminin-coated 6-well plates at a density of 1 x 10^5 cells/well. The cells were cultured in the presence or absence of 1 μM sodium selenite for either 1 or 3 days. To assess the production of ROS, 1.5 μl of the ROS-sensitive dye CellROX DeepRed Reagent (2.5 mM in DMSO; Thermo Fisher Scientific) was added to each well and incubated for 30 min at 37 °C. After removing the growth medium and washing the plates with PBS, the cells were detached with accutase for 3 min at 37 °C. They were then transferred to a falcon tube in 1 ml of PBS, after which a further 2 ml of PBS was added. Following centrifugation, the supernatant was removed, the cells were resuspended in 500 μl PBS and transferred to a FACS tube, whereupon they were immediately placed on ice. Analysis was performed using a FACS Aria II cell sorter (BD Biosciences) and the BD FACS Diva software. Data were analyzed with FlowJo V.10.1 software (TreeStar).

Primary cells

For each experiment, 2 x 8 week-old C57BL/6 mice were killed and their brains immediately removed. The DG were microdissected and dissociated as described above. Following a final wash in Hank's balanced salt solution (HBSS) (PAA; GE Healthcare) the pellet was resuspended in 1 ml of growth medium and filtered through a 40 μm cell sieve (Falcon; BD Biosciences). Cells were plated in 1 ml of neurosphere medium without sodium selenite into 2 wells of a 24-well plate at a density of one DG per well; 0.5 μM sodium selenite was then added to one well, and the cells were incubated at 37 °C for 16 h. CellROX DeepRed Reagent (2.5 mM in DMSO) was added to each well and incubated for 30 min at 37 °C. The cells were transferred to a 15 ml tube and washed with 5 ml of PBS. Following centrifugation, the supernatant was removed, the cells were resuspended in 200 μl PBS. Analysis was performed using a BD FACSCanto cell sorter (BD Biosciences) and the BD FACS Diva software. Data were analysed with FlowJo V.10.1 software. ROS levels following *in vivo* selenium infusion were measured as described above but without the 16 h selenium treatment step.

MitoSOX measurements

For each experiment, 2 x 8 week-old C57BL/6 mice were killed and their brains immediately removed. The DG were microdissected and dissociated as described above. Following a final wash in Hank's balanced salt solution (HBSS) (PAA; GE Healthcare) the pellet was resuspended in 1 ml of growth medium and filtered through a 40 μm cell sieve (Falcon; BD Biosciences). Cells were plated in 1 ml of neurosphere medium without sodium selenite into 2 wells of a 24-well plate at a density of one DG per well; 0.5 μM sodium selenite was then added to one well, and the cells were incubated at 37 °C for 16 h. MitoSOX red reagent (5 mM in DMSO stock) was added to each well to a final concentration of 5 μM and incubated for 10 min at 37 °C. The cells were transferred to a 15 ml tube and washed with 5 ml of PBS. Following centrifugation, the supernatant was removed, the cells were resuspended in 200 μl PBS. Analysis was performed using a BD LSRII cell analyser (BD Biosciences) and the BD FACS Diva software. Data were analysed with FlowJo V.10.1 software.

BrdU and Ki67 immunohistochemistry and quantification of proliferation

To label proliferating cells, mice were given intraperitoneal (i.p) injections of 50 mg/kg BrdU (Sigma); see the experimental design of individual experiments for specific BrdU-labelling paradigms. At the end of the experiment, the animals were perfused with NaCl (0.9 % w/v) and their brains removed and stored in 4 % PFA at 4°C overnight. The next day, brains were transferred to a 30 % sucrose solution for 2–3 d. Coronal sections with a thickness of 40 μm were cut using a sliding microtome (Leica SM2010) cooled with dry ice. Sections were collected and stored as floating sections in cryoprotection solution (CPS) at -20°C. Every sixth section of each brain was pooled in one series for immunohistochemistry. Briefly, brain sections stored in CPS were transferred into PBS and washed. Endogenous peroxidase activity was blocked by adding 0.6 % hydrogen peroxide (Merck Millipore) for 30 min. Sections were rinsed with 0.9 % NaCl. To disrupt hydrogen bonds between bases and to denature the DNA, sections being stained with the BrdU antibody were also treated with pre-warmed 1 M HCl (Emsure) for 30 min at 37°C. After washing, protein-binding sites were blocked with a blocking solution (10 % donkey serum, 0.2 % Triton X-100 in PBS) for 1 h. For quantification of $BrdU^+$ cells, sections were stained for BrdU (anti-rat BrdU, 1:500; AbD Serotec), followed by incubation with an anti-rat-biotin secondary antibody (1:1000; Jackson ImmunoResearch). Ki67 staining was performed with the Ki67 primary (rat anti-Ki67, 1:500; eBioscience) and donkey anti-rat biotin secondary antibodies (1:500; Jackson ImmunoResearch). Detection was performed using the Vectastain ABC-Elite reagent (Vector Laboratories) with diaminobenzidine (Sigma) and 0.04 % NiCl as the chromogen. Sections were mounted onto gelatin-coated glass slides, dried, cleared with Neoclear (Merck) and coverslipped using Neo-mount (Merck). Every sixth section (240 μm apart) was counted in the complete dorsal-ventral extent of the DG, at 40x magnification using a standard brightfield microscope.

CldU and NeuN fluorescence immunohistochemistry and quantification of neuronal survival

To assess survival, mice were injected with CldU (42.5 mg/kg, i.p) immediately following surgery on day 1. Following a 28 d infusion period, mice were perfused with 0.9 % NaCl and the brains removed and sections cut as described above. Sections were first washed with PBS and treated with 0.9 % NaCl, before DNA denaturation was performed in 2 N HCl for 30 min at 37 °C. The sections were then thoroughly washed with PBS and blocked for 1 h in PBS supplemented with 10 % donkey serum (Jackson ImmunoResearch Laboratories) and 0.2 % Triton X-100. Primary antibodies (rat anti-BrdU (1:500; AbD Serotec) and rabbit-anti-NeuN (1:1000; Abcam) were diluted in PBS supplemented with 3 % donkey serum and 0.2 % Triton X-100. Incubation was performed overnight at 4 °C. After several rinses in PBS, the sections were incubated with secondary antibodies (anti-rat Alexa Fluor 488, and anti-rabbit Alexa Fluor 647, 1:1000; Jackson Immunoresearch Laboratories) diluted in PBS supplemented with 3 % donkey serum and 0.2 % Triton X-100 at room temperature for 4 h. They were then washed in PBS, after which DAPI (1:2000) staining was performed for 10 min. After a final wash with PBS, the sections were mounted on glass slides and coverslipped with Aqua-Poly/Mount (Polysciences Europe GmbH). $CldU^+$ cells in every sixth section (240 μm apart) were counted along the complete dorsal-ventral extent of the DG at 40x magnification using a Zeiss Apotome microscope. Results were multiplied by 6 in order to obtain the total number of labelled cells within the DG of each brain. To quantify neuronal survival, 100 randomly selected $CldU^+$ cells per DG were photographed using the apotome function and phenotyped for the co-expression of the neuronal marker NeuN.

BrdU and NeuN fluorescence immunohistochemistry and quantification of neuronal survival in aged animals

To measure net adult neurogenesis in aged animals following a seven-day sodium selenite infusion into the hippocampus, mice were given three i.p. injections of BrdU (50 mg/kg) spaced 6 h apart during the last day of sodium selenite treatment. After a three-week chase period, the mice were perfused with 0.9% NaCl, their brains collected, and coronal sections cut as described above. Immunohistochemistry and quantification of neuronal survival was performed as described above for CldU and NeuN, using mouse anti-BrdU primary antibodies (1:500; Roche) and corresponding anti-mouse Alexa Fluor 568 secondary antibodies (1:1000; Jackson Immunoresearch Laboratories).

CldU and IdU fluorescence immunohistochemistry

To assess whether selenium treatment resulted in recruitment of quiescent NPCs, mice were given three i.p injections CldU (42.5 mg/kg) spaced 6 h apart. One hour after the final CldU injection, the animals received a single i.p injection of either saline or seleno-L-methionine (2 μg/g). Twenty-four hours later, they were administered three i.p injections of IdU (57.5 mg/kg) spaced 6 hours apart, then perfused with 0.9 % NaCl 1 h later. The brains were removed, post-fixed with 4% PFA overnight, followed by 2-3 d in 30% sucrose. Sections were cut as described above. They were then first washed with PBS and treated with 0.9 % NaCl, before DNA denaturation was performed in 1.5 N HCl for 30 min at 37 °C. The sections were thoroughly washed with PBS and blocked for 1 h in PBS supplemented with 10 % goat serum and 0.2 % Triton X-100. Primary antibodies (rat anti-BrdU (CldU, 1:500; AbD Serotec) and mouse anti-BrdU (IdU, 1:1000 BD Biosciences)) were diluted in PBS supplemented with 3 % goat serum and 0.2 % Triton X-100. Incubation was performed overnight at 4 °C. After several rinses in PBS, the sections were incubated with secondary antibodies (goat anti-rat Alexa Fluor 488, and goat anti-mouse Alexa Fluor 568, 1:1000; Jackson Immunoresearch Laboratories) diluted in PBS supplemented with 3 % goat serum and 0.2 % Triton X-100 at room temperature for 4 h. They were then washed in PBS, after which DAPI (1:2000) staining was performed for 10 min. After a final wash with PBS, the sections were mounted on glass slides and coverslipped with Aqua-Poly/Mount (Polysciences Europe GmbH). A total of at least 100 cells in randomly selected fields of view throughout the entire DG were photographed at a 40x magnification using a Zeiss Apotome microscope and were phenotyped as IdU^+CldU^-, IdU^-CldU^+ or IdU^+CldU^+. Further phenotyping of the $CldU^-IdU^+$ cells was performed by staining additional two series of sections. The first antibody combination consisted of the primary antibodies: rat anti-BrdU (CldU, 1:500; AbD Serotec) and mouse

anti-BrdU (IdU, 1:1000 BD Biosciences), rabbit anti-Tbr2 (1:800; Abcam) and goat anti-Sox2 (1:500; R&D Systems), followed by the secondary antibodies: donkey anti-rat Alexa Fluor 594, donkey anti-mouse Alexa Fluor 405, donkey anti-goat Alexa Fluor 488 and donkey anti-rabbit Alexa Fluor 647 (all 1:1000). The second antibody combination consisted of the primary antibodies: rat anti-BrdU (CldU, 1:500; AbD Serotec) and mouse anti-BrdU (IdU, 1:1000 BD Biosciences), rabbit anti-Tbr2 (1:800; Abcam) and guinea pig anti-DCX (1:1000; Millipore), followed by the secondary antibodies: goat anti-rat Alexa Fluor 488, donkey anti-mouse Alexa Fluor 405, goat anti-guinea pig Alexa Fluor 568 and goat anti-rabbit Alexa Fluor 647 (all 1:1000). The staining was performed as described above except for the first antibody combination donkey serum rather than goat serum was used.

Quantitative real-time PCR

Total RNA was isolated from DG and SVZ tissue of 8-week-old female C57BL/6JRj mice using the All prep DNA/RNA/Protein mini kit (Qiagen). 150 ng of total RNA were reverse transcribed using the SensiFAST cDNA synthesis kit from Bioline and the T100 Thermocycler. Quantitative real-time PCR was performed using the SensiFAST SYBR Lo-ROX kit (Bioline). Each cDNA sample (1:10) was amplified using a Thermo Fisher QuantStudio 5 Real-Time PCR System cycler, with primers specific for Sepp1 (Sepp1F 5′-TGTTGAAGAAGCCATTAAGATCG -3′ and Sepp1R 5′- CACAGTTTTACAGAAGTCTTCATCTTC-3′) or LRP8 (LRP8F 5′-AGATGGGCTCAACAGTCACC -3′ and LRP8R 5′- AGTGGGCGATCATAGTTGCT -3′). TATA-binding protein (TBP) was used as control (TbpF 5′-CCAGAACAACAGCCTTCCAC -3′ and TbpR 5′- GGAGTAAGTCCTGTGCCGTA -3). Sepp1 and LRP8 mRNA expression were normalised to TBP RNA expression in each sample. Relative expression values on graphs represent ddCt ($2^{-(dCt_{gene} - dCt_{TBP})}$). Reactions with dH_2O in the absence of any cDNA were included as a negative control.

Inductively coupled plasma-mass spectrometry

Female C57BL/6 mice (8 weeks or 18 months old) were provided with either standard drinking water or water supplemented with seleno-L-methionine (10 ng/μl) for 4 weeks. The mice were then anaesthetised, and blood was collected directly from the heart into EDTA-coated tubes prior to perfusion with 0.9 % NaCl. DG and SVZ tissue were microdissected, snap-frozen and stored at -80 °C until processing. Plasma was prepared by two centrifugation steps at 2000 x g for 15 min. Tissues were sonicated in cold RIPA buffer (Merck) with supernatant collected following centrifugation. Protein levels were quantified with a BCA assay according to the manufacturer's instructions (Thermo Fisher Scientific). Tissue and plasma samples were lyophilised, digested in 25 μl of 65% (v/v) nitric acid (Suprapur, Merck) followed by 25 μl of 30% (v/v) hydrogen peroxide (Suprapur, Merck) and diluted to a final volume of 1 ml using MilliQ-H_2O. Elemental analysis was performed using an Agilent Technologies 8900 Series ICP-QQQ-MS. Iron was monitored at *m/z* 56 using a helium (He) collision gas mode and selenium was monitored at *m/z* 78 and 80 using a mixture of nitrous oxide and hydrogen ($N_2O + H_2$) reaction gas mode, with instrument parameters detailed in Table S1. Plasma metal levels were expressed as a concentration and tissue metal levels were normalised to total protein.

Hippocampal lesion surgery

Mice were anesthetized by an i.p injection of ketamine hydrochloride (100 mg/kg)/ xylazine (10 mg/kg), following which the head was shaved and fixed on the stereotaxic apparatus (David Kopf Instruments). A midline incision was made using a scalpel and the connective tissue was removed using a sterile cotton swab. Two small holes were drilled in the skull over the hippocampus. One microlitre of ET-1 (333 pmol in PBS; Merck) was injected into the right hippocampus while 1 μl of PBS was injected into the left hippocampus at the following coordinates relative to Bregma (anteroposterior: -1.8 mm; mediolateral: ±1.0 mm; dorsoventral: -1.7 mm). A pulled borosilicate glass micropipette (1/0.58 mm outer/inner diameter; World Precision Instruments) attached to a 5 μl Hamilton syringe was used for the injection. To reduce backflow, all injections were performed over 5 min and the pipette was left in place for 10 min before being slowly withdrawn over 2 min. Sham surgery was performed by bilateral injection with PBS. The incision was closed using 5-0 nylon sutures (Ethicon). After the surgery and for the following 2 days, the mice were given an i.p injection of the analgesic buprenorphine (2 mg/kg; Fort Dodge, Provet) and the antibiotic enrofloxacin (5 mg/kg; Bayer). Animals were kept in a humidified chamber at 28 °C for 48 h, after which they were housed at room temperature.

Running distance tracking

Voluntary wheel running was monitored using a stable magnetic reed switch attached to a digital odometer (Cat eye Enduro 8) and a magnet fixed to a hanging running wheel (Labodia; 11 cm in diameter). For the tracking, 8-week-old *Sepp1* KO or *LRP8* KO mice and their WT littermates were single housed and habituated to the cages with running wheel one day prior to recording. Running distance, elapsed running time, maximum speed and average speed were recorded daily.

Behavioral testing

All behavioral tests were performed during the light period between 9am and 6pm and the apparatus was carefully cleaned by wiping with 70% ethanol after each trial to remove the olfactory cues. All mice were familiarized with the researchers and habituated to the training room prior to the experiment. The animals to be tested were moved into the behavioral testing room 30 min before the start of the trial, to limit olfactory cues. The bedding of the animal's home cage was not changed during the period of the behavioral tests. To minimize the difference made by experimenter handling, mice were handled by the same experimenter throughout all behavioral experiments.

Active place avoidance test

Mice were placed on a gridded platform (1 meter diameter) that rotated at 1 revolution per min (Biosignal). A 5 min habituation session with no shocks was conducted on the first day, with 10 min testing sessions being conducted on each of the following 4 or 5 days. During the testing sessions, a 60° shock zone was defined by the tracking computer, and if an animal entered this exclusion area it received a 0.5 mA foot shock with a 500 ms latency. The inter-shock latency was 1,500 ms. Four visual cues were spaced evenly around the room and the animal was placed into the arena at the same starting location on each day of testing. At the conclusion of testing, the mice were randomly assigned to control or selenium treatment groups. Following 4 weeks of saline or selenium treatment (10 μg/ml in drinking water) the animals were retested on the APA task. During the retesting phase, the shock zone location remained the same, but the visual cues were replaced with novel cues. Data was collected using a ceiling-mounted video camera. Between testing of each animal, the grid and platform were thoroughly cleaned with 70 % ethanol. Parameters including total distance travelled, number of shocks received, first and second time to receive a shock and maximum time spent avoiding the shock zone were all recorded automatically. Learning ability during the testing period was also examined by comparing the parameters on the first day to those on the fourth or fifth day of testing for each animal and represented as a percentage improvement during the task.

Barnes maze

The testing room was 2 m^2 in size and the Barnes maze (32 holes and 1 m in diameter in size) was placed on a pedestal in the middle of the room at a height corresponding to four high-contrast visual cues, one in the middle of each of its four walls. The light intensity in the room was set to 1000 lux at the surface of the maze, encouraging the mice to find shelter in a darkened escape box, which was located under one of the holes. During habituation to the maze, the animals were first placed into the escape box containing a fresh tissue for 1 min. They were then placed into the center of the maze and were allowed to explore the area for 5 min or until they had entered the escape box. Animals which did not locate the escape box were carefully placed into it and allowed to rest there for 20 s. The mice were then placed back into their home cage. Between each mouse, the maze, as well as the escape box, were thoroughly cleaned with 70% ethanol and the escape box equipped with a fresh tissue. On the first day of testing, the escape box was rotated 90 degrees from the location of the habituation and remained there for all testing days. Each testing day comprised three individual trials, which were conducted at least 1.5 h apart. For each trial, the mice were gently placed into a darkened start chamber and placed into the center of one of the four maze quadrants for 15 s. To minimize any location bias, the starting quadrant for each mouse was rotated by 90 degrees in each subsequent trial. The trial commenced following removal of the start chamber. The mice were given 3 min to locate the escape box. The trial finished once an animal had entered the escape box or after 3 min had elapsed. If an animal failed to find the escape box, it was placed into the box and allowed to rest there for 20 s. After the trial, the mice were placed back into their home cage. A tracking computer together with a ceiling-mounted video camera were used to collect visual data of the animals during the trial. Data were analyzed using the Ethovision XT14 software to assess primary latency to the escape box, escape latency upon entering the escape box and general movement parameters.

Open field test

Spontaneous activity and anxiety-like behaviors in the open field were tested using an opaque plastic cube box (30 × 30 × 30 cm) under a camera; the center region was defined as a 15 cm × 15 cm area. To reduce anxiety in the animals, the light intensity in the center of the box was set to 100±5 lux. Each mouse was first placed in the center of the box and given 20 min to move freely in the box. Total distance travelled and the distance travelled in the center were recorded and analyzed using the Noldus video tracking system (Ethovision XT 14).

Novel object recognition test

The novel object recognition (NOR) test was carried out to assess the long-term recognition memory. Each trial consisted of a familiarization session and a test session. In the familiarization session, each mouse was placed into a testing box (45 × 45 × 30 cm); to reduce anxiety in the animals, light intensity in the center of box was set to 100±5 lux. The mouse was allowed to explore freely for 10 min in the box which contained two identical objects (5 ×5 × 5 cm) at symmetrically diagonal positions. Twenty-four hours later, one familiar object in the box was replaced with a novel object of the same size but different brightness, shape and texture. In the test session, the mouse was placed back into the box and given 10 min to explore the two objects. Animals that remembered the familiar object spent more time exploring the novel object. The activity of the mice was recorded using a Noldus video tracking system (Ethovision XT 14). The time spent sniffing and exploring the novel object was recorded as the period when the tip of the snout was in close proximity to the object (distance between the nose and the object was less than 2 cm). The exploration index was defined as the ratio of exploration duration around two objects over the entire duration of the familiarization session while the discrimination index was defined as the ratio of exploration duration around the novel object over the duration around both the objects in the test session.

Novel object location test

The novel object location (NOL) test is a spatial variant of the NOR test which allows measurement of the memory of spatial location due to the animals ability to encode both the feature of the object and the spatial location information(Massey et al., 2003). In this paradigm, two identical and familiar objects were presented in the familiarization session with one object shifting to a novel location 24 h later for the test session. The exploration and discrimination index were measured as described above.

Contextual fear conditioning

Fear conditioning is a Pavlovian learning paradigm that has been widely used in different species to evaluate associative learning ability(Curzon et al., 2009). In this test, animals need to associate a conditioned stimulus (CS), a unique context, with a noxious unconditioned stimulus (US), an electrical shock. If they succeed in remembering and associating the novel environment with the shock, they will demonstrate a freezing response once returned to the same environment.

Contextual fear conditioning was performed in individual soundproof operant chambers with plastic walls and a wire grid floor, which were scented with lemon essence and cleaned with hot water and ethanol between animals. Mice spent a total of 8 min in the apparatus, with four footshocks (1 s, 0.8 mA) being delivered at 2, 4, 6 and 8 min. Recall tests were performed 24 h after fear conditioning, by returning the mice to the apparatus for 4 min in the absence of foot shocks. The percentage of time spent freezing during the 4 min recall test was measured. Data were analyzed using FreezeFrame 4 (Actimetrics) by a researcher blind to the treatment group of the mice.

Y-maze

To assess long-term spatial memory with minimal stress, the forced alternation test was conducted using a Y-maze apparatus composed of three arms made of transparent plastic joined in the middle to form a Y shape. The insides of each arm were identical, providing no intramaze cues. Each arm of the Y-maze was 40 cm long, 9 cm wide, and 17 cm high. Unique visual cues were attached to the outside of each arm, allowing mice to identify the difference between arms. This test is based on animals' innate curiosity to explore a novel area. To reduce anxiety in the animals, the light intensity in the centre of Y-maze was set to 100±5 lux.

Mice were placed into one of the arms (start arm) and allowed to freely explore the maze for 5 min with one of the arms closed by an opaque guillotine door so that they could not observe the visual cue on the closed arm (training trial). After a 24 h interval, the guillotine door was removed, and mice were returned to the Y-maze. The animals were placed into the start arm and allowed to access all three arms of the maze for 5 min (test trial). The video was recorded by a monitor directly above the apparatus during the test trial. The total distance travelled, average speed, number of entries into and time spent in each arm in the test trial were analyzed using the Noldus video tracking system (Ethovision XT 14). If a mouse climbed on the maze wall, it was immediately returned to the maze arm. An arm entry was recorded when 85% of a mouse's body had entered the arm.

QUANTIFICATION AND STATISTICAL ANALYSIS

Data analysis was performed using Prism software (Version 9, GraphPad Software). Results were expressed as mean ± standard error of the mean (SEM). Statistical significance was determined using a Student's t test when the experiment contained two groups, or ANOVA when comparing more than two groups. Post-hoc analysis was performed on the ANOVA using the Dunnett, Tukey's or Sidak post hoc tests as described in the figure legends. Prior to analyzing the statistical significance of differences among treatments, we tested whether the variance was similar using either the F-test or Bartlett test. The level of conventional statistical significance was set at $p < 0.05$. The statistical parameters can be found in the figures and the figure legends.